A Flexible Model for Spatial Volatility with an Application to the Chicago Housing Market *

Jiyoung Chae †

August 11, 2020

Abstract

Existing volatility models normally emphasize the behavior of prices in a *temporal* sense and comparatively few studies have explicitly analyzed the spatial variation of volatility. This paper proposes a flexible *spatial* volatility model for squared returns using a Box-Cox transformation that includes the linear and log-linear forms as special cases, thus providing a unified framework for simultaneously testing space-varying volatility and its functional form. The maximum likelihood method is used to estimate the model and Monte Carlo simulations are conducted to investigate the finite sample performance of the maximum likelihood estimator. The use of the model is also illustrated by a substantive application to housing price data in the city of Chicago. The estimation results suggest that housing returns in Chicago show the volatility exhibits strong spatial dependence and the log-linear functional form is appropriate. In the final log-linear model, a new practical indicator, called *neighborhood elasticity*, is proposed that determines how volatility in one neighborhood is linked to that in surrounding neighborhoods. From a practical point of view, this indicator provides a tool to help policy-makers mitigate volatility transmission and the risk of contagion in the housing market.

Keywords: Spatial volatility clustering, Spatial dependence, Maximum Likelihood, Monte Carlo simulation

JEL Classification: C13, C21, C49, C55, R39

*I am extremely grateful to my advisor Anil K. Bera for his invaluable guidance and support. I also appreciate my committee members, Geoffrey J. D. Hewings, Daniel McMillen, and JiHyung Lee, for their insightful conversations and feedback. This paper has also benefited from comments and suggestions by Amit Batabyal and Pavel Krivenko at the Mid-Continent Regional Science Association (MCRSA 2019) Conference in Madison, Wisconsin, and my mentor, Xu Lin, at the Annual Meeting of the Midwest Econometrics Group (MEG 2019) in Columbus, Ohio. I gratefully acknowledge the financial support provided by Illinois REALTORS® to the Regional Economics Applications Laboratory (REAL) that provided research funding. All errors are mine.

†Department of Economics, University of Illinois at Urbana-Champaign, Urbana, IL 61801, USA. Email: jchae3@illinois.edu.

1 Introduction

The volatility of housing prices has important implications for household behavior and welfare as well as for the aggregate U.S. economy. At the household level, it can be easily argued that housing is the most important asset for many households. It is usually both the largest asset they own and the most readily available source of collateral against which they can borrow.[1] Higher housing price volatility thus has the potential to pose substantial risk to household welfare. For example, it could distort a household's housing choices, lead to a higher likelihood of mortgage foreclosure, and also affect home building and intergenerational equity (Miller and Peng, 2006; Oxley and Haffner, 2010; Stephens, 2011). From a macroeconomic perspective, the impact of housing price volatility is similarly damaging as the housing sector is vital to the national economy. Recent experience has made painfully clear the importance of the housing market in the U.S. A catastrophic and systematic collapse of the U.S. housing market triggered an economic recession, the so-called Great Recession, that rippled throughout the global economy.

The level of housing price volatility is more important today than ever, as more U.S. households are headed by renters (and therefore housing investors) than at any point since at least 1965. According to a Pew Research Center analysis of Census Bureau housing data in 2017, the number of households renting their homes increased significantly, from 31.2% in 2006 to 36.6% in 2016, near the high of 37% in 1965.[2] The analysis also states that, in 2016, 65% of the nation's households headed by people under age 35 are rental households. This indicates that higher housing price volatility levels may discourage newly formed households from committing to homeownership as they view housing as a risky investment vehicle, although previously housing was perceived as a stable investment and a reliable inflation hedge (Stevenson, 1999; Anari and Kolari, 2002).

Research into housing price volatility has received increased attention in the housing literature in recent years. Much of this research has focused primarily on investigating whether housing price volatility is *time-varying*, i.e., housing prices exhibit volatility clustering or autoregressive conditional heteroskedasticity (ARCH) effects (e.g. Dolde and Tirtiroglu, 1997; Crawford and Fratantoni, 2003; Miller and Peng, 2006; Miles, 2008; Barros et al., 2015). While it is widely recognized that conditional heteroskedasticity is pervasive in studies of housing price volatility, there has been little research addressing such heteroskedasticity in the context of *spatial volatility*.

Unlike previous housing-market cycles, the most recent cycle has been the longest in history, spanning well over a decade. During this period, market fundamentals, such as income, employment, population and net

[1] According to the Federal Reserve's 2016 Survey of Consumer Finances (SCF), at $24.2 trillion, the primary residence accounted for about one quarter of all assets held by households in 2016. The survey also reveals that the value of the primary mortgage debt was the largest liability faced by the homeowners. `https://www.federalreserve.gov/econres/scfindex.htm`

[2] Cilluffo et al. (2017).

immigration, have grown at different rates throughout the country and thus have increasingly been exposed to regional differentials. Therefore, housing price volatility has come to differentially affect parts of the U.S. in a way that it did not before. In order to see the spatial variation of volatility in the local housing market in the U.S., consider the annual return on housing in 2017 at the census tract level in Chicago. Construction of the return data is described in Section 5. Looking at the representative spatial plot for the returns and squared returns as a volatility proxy in Figure 1, it is evident that, while returns appear to be randomly distributed over space, squared returns are spatially correlated, with distinct clusters of high and low volatility readily identifiable, e.g., high volatility clusters are detected in Chicago's west-side neighborhoods (Austin (23); West Garfield Park (26) and East Garfield Park (27); North Lawndale (29) and South Lawndale (30)) and south side neighborhoods (South Chicago (46); West Englewood (67) and Englewood (68); Greater Grand Crossing (69); Auburn Gresham (71)).[3]

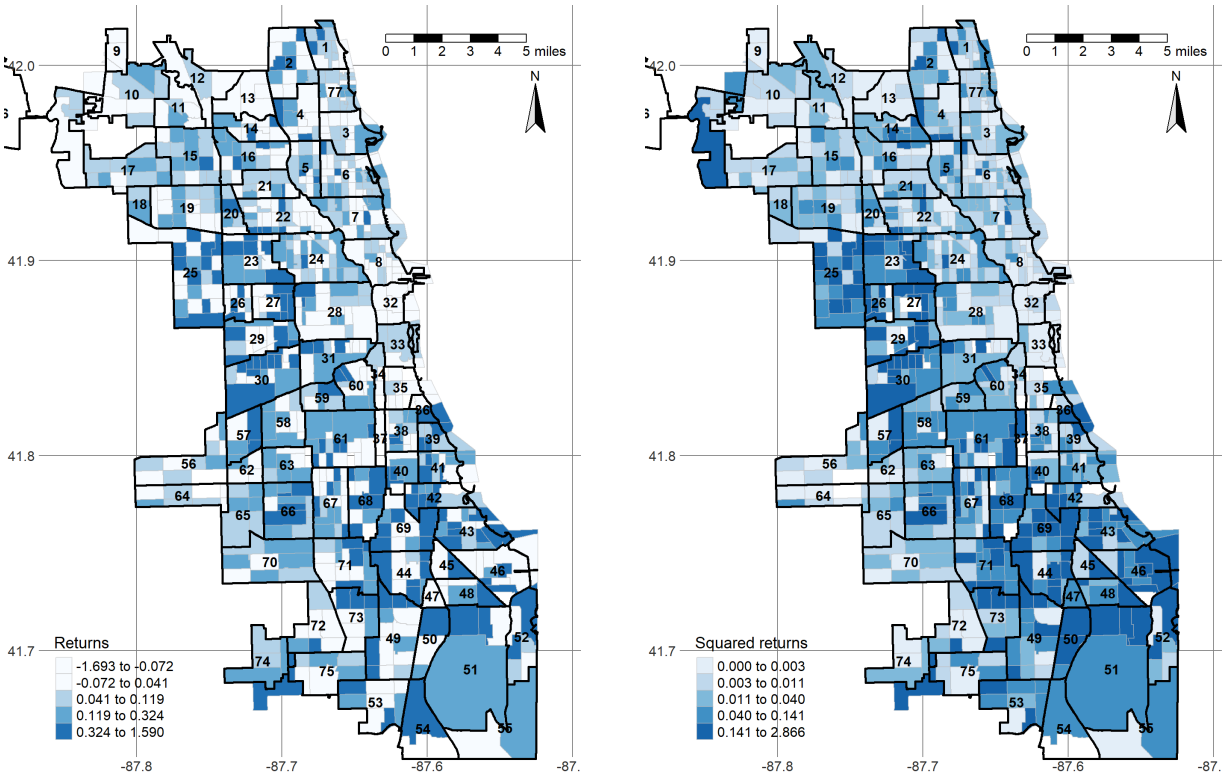

(a) Returns (b) Squared returns

FIGURE 1 Spatial distribution of (a) returns and (b) squared returns, 2017

Note: The above figure shows the spatial distribution of returns and squared returns by census tract in the city of Chicago for 2017. The listed numbers refer to the codes for Chicago community areas (see Table 13 in the Appendix for details).

Shifting the 2D view to the 3D map view given in Figure 2, it can be easily seen that clusters of high volatility are more pronounced in the southern part of the Chicago. This clustering pattern may occur in any housing market, as the nature of change in the U.S. housing market has opened significant gaps between regions in recent

[3]This pattern is also detected when using an alternative measure of volatility, absolute returns, suggesting that the dependence behavior is not sensitive to the choice of a particular measure of volatility. Robust analysis using this alternative is addressed in Section 6.

decades.

Motivated by the visual implications of Figure 1 and Figure 2, this paper develops a spatial ARCH-type model of squared returns to examine housing price volatility in the context of a spatial regression framework.[4] Specifically, the proposed model incorporates space-varying volatility (or spatial volatility clustering), which is the spatial equivalent of time-varying volatility in a time-series context.

When analyzing economic data that take only positive values, the use of transformations is very common and may be helpful when the usual assumptions are not satisfied in one's original model. In the finance literature, the logarithmic transformation of realized volatility (the sum of squared intraday returns) is often used in empirical applications owing to its superior finite sample properties. Barndorff-Nielsen and Shephard (2005) demonstrate that the finite sample distribution of the log transformation of realized volatility is closer to the asymptotic standard normal distribution than to the raw version of realized volatility. Most empirical studies have also focused on the log transformation in volatility estimation and forecasting (Andersen et al., 2001; Corsi, 2009; Hansen et al., 2012; Koopman and Scharth, 2012).

Recently, however, a more flexible power transformation suggested by Box and Cox (1964) has been considered in this context (Gonçalves and Meddahi, 2011; Nugroho and Morimoto, 2016; Weigand, 2014; Zheng and Song, 2014; Taylor, 2017). The Box-Cox transformation indexed by the transformation parameter defines a general class of functional forms that includes the linear and log-linear forms as special cases. This feature allows the data added flexibility in model specification and provides a unified structure for statistically distinguishing between alternative functional specifications.

Although the Box-Cox transformation has long been applied in finance, including to return-based volatility models, there has been almost no attempt to introduce the transformation in the spatial context. Studies conducted by Baltagi and Li (2004) and Li and Le (2010) are the most similar to the present paper, in that both explicitly consider functional form and spatial dependence simultaneously by applying the Box-Cox transformations in the context of the spatial regression model. In the former study, Baltagi and Li (2004) derive Lagrangian multiplier (LM) tests. In the latter study, the framework builds on double-length regression (DLR). Both of these studies indicate that choosing the correct functional form is beneficial in the presence of spatial dependence.

In light of the foregoing, this paper generalizes the spatial ARCH model to a more general version with the Box-Cox transformation to derive the most appropriate functional form of spatial volatility, where the linear and log-linear models are special cases (hereafter referred to as the BC-SARCH model). The advantages of the BC-SARCH model are that both functional form and spatial dependence can be considered simultaneously,

[4] As indicated by Bollerslev et al. (1992), squared returns of not only exchange rate data but of all speculative price series typically exhibit volatility clustering and ARCH-type models are appropriate for volatility estimations.

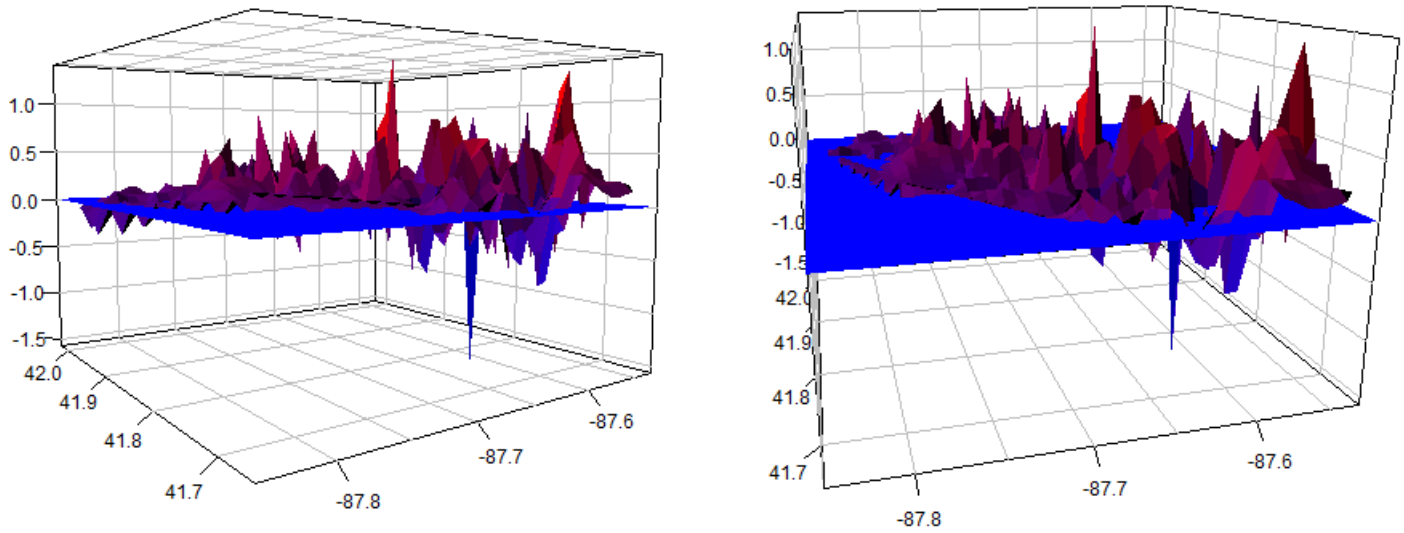

(a) Returns

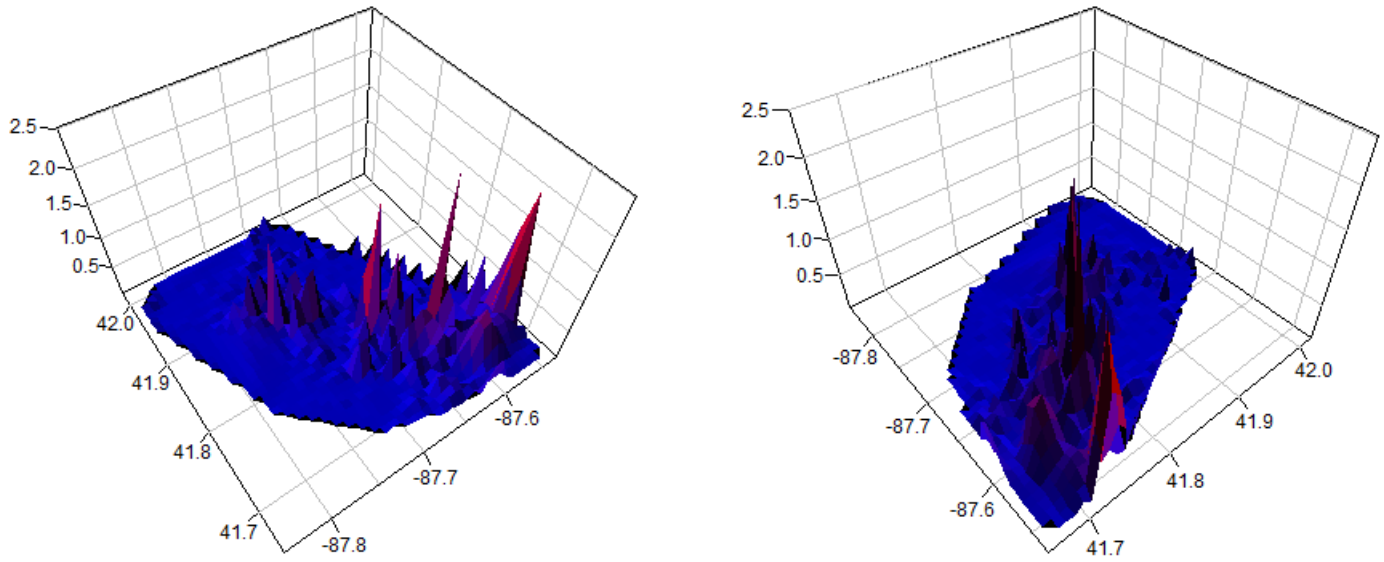

(b) Squared returns

FIGURE 2 Spatial distribution of returns and squared returns, 2017

and that the validity of linear or log-linear specifications can be addressed. The proposed model would also be useful in another respect, in that the transformation might affect the distributional shape of the variable favorably. It is well known that the unconditional distribution of data for which typical linear models are used is frequently skewed and leptokurtic. Given that appropriate transformation may induce symmetry to the distribution, it seems probable that the proposed model would yield, apart from capturing the presence of spatial dependence, approximate symmetric and mesokurtic properties (i.e., normality) for the unconditional distribution.

To estimate the BC-SARCH model, a maximum likelihood estimation (MLE) procedure is applied to both simulated and empirical data. The finite sample properties of the estimator is examined in a Monte Carlo experiment and the result suggests that the MLEs perform well in estimating parameters of interest. This study also carries out a detailed empirical analysis using housing sales price data within the city of Chicago in a period running from 2009 through 2018. It uses squared returns of observed housing sales prices that serve as a proxy for latent volatility and ensures that the study period covers the latest dynamics in the Chicago housing market. In this empirical application of the BC-SARCH model, the results suggest that volatility exhibits substantial spatial dependence and its functional form is close to the log-linear model. Judging by the associated model diagnostics and specification tests, the log-linear model is found to be superior to the linear model. Furthermore, the resulting spatial dependence parameter in the log-linear model serves as *neighborhood elasticity*, which measures how volatility in one neighborhood is linked to that in surrounding neighborhoods. For 2009 through 2018, the average value of the cross-sectional neighborhood elasticity is observed to be around 0.4, indicating that a 1% increase in volatility determines an increase of 0.4% in the volatility of neighboring locations. This analysis is further extended to the spatial panel data models to test temporal heterogeneity in neighborhood elasticity, i.e., whether neighborhood elasticity stays the same over time. Applying the method introduced by Xu and Yang (2019), this paper shows that, after controlling for both spatial and temporal heterogeneity in intercepts, neighborhood elasticity is homogeneous and there exists no structural change.

This paper contributes to the existing literature methodologically and empirically. The methodological contribution consists of a unified structure for statistically testing both spatial dependence and functional form simultaneously. Another methodological contribution involves the use of adjusted quasi score (AQS) tests for testing the existence of temporal heterogeneity in spatial parameters in spatial panel data models, a method that was recently developed by Xu and Yang (2019) that has not been used previously in the literature. The empirical contribution relates to the use of the most recent multiple listing service (MLS) price data, allowing extension of spatial volatility analysis at a finer spatial scale (the census-tract scale). As noted above, while the spatial dependence of housing price volatility has been detected at large spatial scales (the state or MSA scale), a rigorous empirical examination of the linkage at a much smaller spatial scale has not been carried out

because of the lack of publicly available data.[5] Finally, a new practical indicator, neighborhood elasticity, is proposed that can serve as a tool for policy-makers to assist them to mitigate volatility transmission and the risk of contagion in the housing market.

The rest of this paper is organized as follows. In Section 2, I review the related literature on spatial volatility models. In Section 3, I discuss the detailed description of the BC-SARCH model under consideration. The Monte Carlo simulation experiment is conducted in Section 4 to evaluate the finite sample performance of the MLEs for the proposed model. In Section 5, I describe the data used in this paper and associated estimation results. In Section 6, I verify the robustness of the findings in alternative modeling choices. Section 7 concludes with a discussion of the contributions of this paper, and implications for public policy.

2 Related Literature

An increasing amount of studies have attempted to model the housing price volatility of individual housing markets by employing the class of generalized autoregressive conditional heteroskedasticity (GARCH) models. Earlier studies have employed different univariate GARCH-type models, such as GARCH and GARCH-in-Mean (GARCH-M) (e.g. Dolde and Tirtiroglu, 1997; Stevenson et al., 2007; Hossain and Latif, 2009), exponential GARCH (EGARCH) and exponential GARCH-in-Mean (EGARCH-M) (e.g. Lee, 2009; Willcocks, 2010; Lin and Fuerst, 2014), component GARCH (CGARCH) and component GARCH-in-Mean (CGARCH-M) (e.g. Miles, 2011; Lee and Reed, 2013; Karoglou et al., 2013).

Nevertheless, there remains a lack of statistical models accounting for the spatial conditional heteroskedasticity in a spatial econometric context, despite the growing body of evidence that neighborhood plays an important role in volatility dynamics as mentioned in the introduction. Subsequent to the pioneering work of Bera and Simlai (2005), who propose a special type of spatial ARCH (SARCH) model by employing the information matrix (IM) test statistic in a simple SAR model, several ARCH or GARCH-type models have been proposed to incorporate both temporal and spatial effects in the dynamics of volatility. For example, Borovkova and Lopuhaa (2012) and Caporin and Paruolo (2006) introduce a temporal GARCH model, which includes temporal lags influenced by neighboring observations, while Otto et al. (2018) introduce an exponential SARCH model and illustrate the use of model as a residual process for the spatial modeling of lung cancer mortality in U.S. counties. Very recently, Sato and Matsuda (2020) suggest a further extension of SARCH models with applications to land prices in the Tokyo area of Japan. On the other hand, several recent papers have discussed moment methods of spatial econometric models with heteroskedasticity (e.g. Breitung and Wigger, 2018; Taşpınar et al., 2019).

[5] Although Bera and Simlai (2005) use data from 506 census tracts in the Boston metropolitan area, the data are taken from the 1970 census, which does not reflect recent housing cycles.

Interestingly, in spite of this promising start, the use of a spatial econometric approach to detect the presence of conditional spatial volatility has remained largely unexplored in the literature. Furthermore, it is not yet established which functional form is the most appropriate for evaluating space-varying volatility in the housing market.

3 The Model and Econometric Methodology

The most widely used model for describing nonlinear dependencies of returns in a time-series context is the ARCH class of models, where past squared returns are used to predict subsequent squared returns. This approach potentially suggests that, in a spatial context, squared returns can be described by the squares of neighboring observations. The simplest specification for approximating this expectation relates the squared returns in one location to the weighted average of the neighboring squared observations. To specify the functional relationship, the following BC-SARCH model is proposed, which is expressed as

$$\frac{(y_i^2)^\lambda - 1}{\lambda} = \alpha_0 + \alpha_1 \sum_{j \neq i}^{n} w_{ij} \frac{(y_j^2)^\lambda - 1}{\lambda} + \epsilon_i, \tag{1}$$

where y_i^2 are squared returns at location i, y_j^2 are the values of the variable at surrounding locations j ($j \neq i$), w_{ij} are the spatial weights, which are non-zero when i and j are neighbors and zero otherwise, and $\epsilon_i \sim IIDN(0, \sigma^2), i = 1, 2, ..., n$. It is important to note that no exogenous variables are introduced in this model as typical hedonic pricing variables (e.g., structural or neighborhood attributes of housing) were found insignificant mostly in the previous analysis. Equation (1) can be also expressed using the matrix form by letting $y^2 = (y_1^2, y_2^2, ..., y_n^2)'$ be the data on which the Box-Cox transformation is applied.

$$y^{2(\lambda)} = \alpha_1 W y^{2(\lambda)} + \alpha_0 \mathbf{1} + \epsilon, \tag{2}$$

where $y^{2(\lambda)}$ is the Box-Cox transformation of y^2, W is a row-normalized spatial weight matrix such that $\sum_{j \neq i}^{n} w_{ij} = 1$ for all i, with zeros on the main diagonal, the off-diagonal elements take values between 0 and 1, and $\mathbf{1}$ is an n-dimensional vector of ones.

The Box-Cox model in equation (1) clearly reduces to the linear model when $\lambda = 1$, and to the log-linear

model when $\lambda \to 0$, such that

$$f(y_i^2) = \begin{cases} y_i^2 = \alpha_0 + \alpha_1 \sum_{j \neq i}^{n} w_{ij} y_j^2 + \epsilon_i & \text{when } \lambda = 1 \quad (3) \\ \log y_i^2 = \alpha_0 + \alpha_1 \sum_{j \neq i}^{n} w_{ij} \log y_j^2 + \epsilon_i & \text{when } \lambda \to 0, \quad (4) \end{cases}$$

and thus tests of λ aid in selecting the proper functional form. The log-linear form in equation (4) is prevalent in demand studies and the coefficients can be interpreted as elasticities of demand. For example, let $\log Q = \alpha_0 + \alpha_1 \log P + \epsilon$ denote the traditional demand function with respect to price; the coefficient $\alpha_1 = \frac{\partial \log Q}{\partial \log P}$ is then a price elasticity of demand which represents the percentage change in demand with respect to a 1% change in price. Similarly, the parameter estimate of α_1 in equation (4) amounts to an elasticity, but one that is conditional on neighborhood information $\mathbb{N}$. To see this, let the conditional expectation of equation (4) be given by $E[\log y_i^2|\mathbb{N}] = \alpha_1 Z_i$ where $Z_i = \sum_{j \neq i}^{n} w_{ij} \log y_j^2$, the neighborhood average. This in turn leads to

$$\frac{\partial E[\log y_i^2|\mathbb{N}]}{\partial Z_i} = \alpha_1, \quad (5)$$

which measures the sensitivity of the expected volatility at location i to an increase in volatility of the neighborhood, and it will be convenient to call it the *neighborhood elasticity*.

A heuristic justification of the BC-SARCH model presented in equation (1) can be provided as follows. It begins with the idea of the constant elasticity of substitution (CES) production function introduced by Solow (1956) and later expanded on by Arrow et al. (1961). Consider the following CES-type volatility production function consisting of two inputs, autonomous variance σ^2 and neighborhood-induced variance $y_j^2, j \neq i$ (combined as $\sum_{j \neq i}^{n} w_{ij} (y_j^2)^\lambda$), conditional on all neighborhood $\mathbb{N}$ with $E(y_i|\mathbb{N}) = 0$. Then,

$$V(y_i|\mathbb{N}) = E(y_i^2|\mathbb{N}) = \left[\alpha_0 (\sigma^2)^\lambda + \alpha_1 \sum_{j \neq i}^{n} w_{ij} (y_j^2)^\lambda \right]^{\frac{1}{\lambda}}, \quad (6)$$

where α_0 and α_1 are the share parameters with $\alpha_0 + \alpha_1 = 1$, and λ is the substitution parameter that can be used to derive the elasticity of substitution $\eta = \frac{1}{1-\lambda}$. This function indicates that, for $\alpha_1 = 0$, aggregate variance will be determined only by an exogenously given level of autonomous variance σ^2, both conditionally and unconditionally, as α_0 becomes 1 and λ cancels out. The function also nests several well-known functional forms as special cases, depending on the value of the substitution parameter λ; for $\lambda \to 0$, η approaches 1 and the CES turns to the Cobb-Douglas form; for $\lambda \to -\infty$, η approaches 0 and the CES becomes the Leontief or perfect complements production function; and for $\lambda \to 1$, η approaches infinity and the CES becomes a linear

or perfect substitutes production function.

Subtracting 1 from both sides of equation (6) and dividing by the substitution parameter λ yields

$$\begin{aligned}\frac{E(y_i^2|\mathbb{N})^\lambda - 1}{\lambda} &= \frac{\alpha_0(\sigma^2)^\lambda}{\lambda} + \frac{\alpha_1 \sum_{j\neq i}^n w_{ij}(y_j^2)^\lambda}{\lambda} - \frac{1}{\lambda} \\ &= \alpha_0\frac{(\sigma^2)^\lambda - 1}{\lambda} + \alpha_1 \sum_{j\neq i}^n w_{ij}\frac{(y_j^2)^\lambda - 1}{\lambda} - \frac{1}{\lambda} + \frac{\alpha_0}{\lambda} + \frac{\alpha_1}{\lambda} \quad \text{since } \sum_{j\neq i}^n w_{ij} = 1 \\ &= \alpha_0\frac{(\sigma^2)^\lambda - 1}{\lambda} + \alpha_1 \sum_{j\neq i}^n w_{ij}\frac{(y_j^2)^\lambda - 1}{\lambda} \quad \text{since } \alpha_0 + \alpha_1 = 1,\end{aligned}$$

and thus,

$$E\left[\frac{(y_i^2)^\lambda - 1}{\lambda}\middle|\mathbb{N}\right] = \alpha_0\frac{(\sigma^2)^\lambda - 1}{\lambda} + \alpha_1 \sum_{j\neq i}^n w_{ij}\frac{(y_j^2)^\lambda - 1}{\lambda}, \tag{7}$$

which is essentially the same as the proposed model in equation (1). Therefore, when $\lambda = 1$, it becomes the linear specification with some constant $\alpha_0(\sigma^2 - 1) = \alpha_0'$ and when $\lambda \to 0$, it is log-linear with some constant $\alpha_0 \log \sigma^2 = \alpha_0'$. Note that equation (6) is not exactly a CES function, but it provides some intuitive support for the BC-SARCH model.

The process of choosing the appropriate functional form for the BC-SARCH models involves maximizing a log-likelihood function. The likelihood function, in terms of the original variable, is expressed by

$$L(\theta|y^2) = \frac{1}{\sqrt{(2\pi\sigma^2)^n}} \exp\left\{-\frac{\epsilon'\epsilon}{2\sigma^2}\right\} J, \tag{8}$$

where θ is a vector of parameters, $\epsilon = (I - \alpha_1 W)y^{2(\lambda)} - \alpha_0 \mathbf{1}$ with $\mathbf{1}$ denoting the $n \times n$ identity matrix, and J is the Jacobian of the transformation from ϵ to y^2, or

$$J = \left|\frac{d\epsilon}{dy^{2(\lambda)}}\frac{dy^{2(\lambda)}}{dy^2}\right| = |I - \alpha_1 W| \prod_{i=1}^n \left(y_i^2\right)^{\lambda-1}. \tag{9}$$

Consequently, the log-likelihood function is given by

$$\log L(\theta|y^2) = -\frac{n}{2}\log(2\pi) - \frac{n}{2}\log(\sigma^2) - \frac{\epsilon'\epsilon}{2\sigma^2} + \log|I - \alpha_1 W| + (\lambda - 1)\sum_{i=1}^n \log\left(y_i^2\right). \tag{10}$$

Note that $\log|I - \alpha_1 W| = \sum_{i=1}^n \log(1 - \alpha_1\omega_i)$, where the ω_i's are the eigenvalues of W; see Ord (1975) and Anselin (1988). By assumption, the matrix $I - \alpha_1 W$ is nonsingular. The last term in equation (10) vanishes in the case of the linear model.

Finally, the log-likelihood function is maximized with respect to the parameter vector $\theta = \{\alpha_0, \alpha_1, \lambda, \sigma^2\}$ to obtain the maximum likelihood estimators (MLEs). The maximization is performed numerically by using the first derivatives (gradient) with respect to the parameter θ, which can be obtained from equation (10) as follows:

$$\frac{\partial \log L}{\partial \alpha_0} = \frac{1}{\sigma^2}\mathbf{1}'\epsilon \tag{11}$$

$$\frac{\partial \log L}{\partial \alpha_1} = \frac{1}{\sigma^2}(Wy^{2(\lambda)})'\epsilon - \sum_{i=1}^{n}\frac{\omega_i}{1-\alpha_1\omega_i} \tag{12}$$

$$\frac{\partial \log L}{\partial \lambda} = -\frac{1}{\sigma^2}\left[(I-\alpha_1 W)\frac{\partial y^{2(\lambda)}}{\partial \lambda}\right]'\epsilon + \sum_{i=1}^{n}\log\left(y_i^2\right) \tag{13}$$

$$\frac{\partial \log L}{\partial \sigma^2} = -\frac{n}{2\sigma^2} + \frac{1}{2\sigma^4}\epsilon'\epsilon, \tag{14}$$

where $\frac{\partial y^{2(\lambda)}}{\partial \lambda} = \frac{\lambda y^{2\lambda}\log y^2 - y^{2\lambda}+1}{\lambda^2}$. The second derivatives (Hessian) of the log-likelihood function are given in the Appendix where they are used to obtain the standard errors of the model parameters.

It is important to note that the asymptotic distribution of the MLEs are not formally established in the paper but are likely to hold under similar sets of assumptions developed by Lee (2004), who presents a comprehensive investigation of the asymptotic properties of the MLEs widely used in the literature to estimate spatial models.

4 Monte Carlo Simulation

4.1 Experimental Design

In this section I present a Monte Carlo experiment to evaluate the empirical evidence pertaining to the spatial regression using the BC-SARCH specification in a simulated setting. It has been argued in the literature that a spatial regression with heteroskedastic innovation can lead to significantly biased ML estimators (Kelejian and Prucha, 2010). A recent study by Piras and Prucha (2014) points out that the finite sample properties are crucial for understanding bias for estimators of various spatial models. Following the lead provided by the existing literature, I investigate the finite sample performance of the BC-SARCH estimators of interest.

In all of the experiments, the data-generating process is assumed to be of the form specified in equation (1). The spatial weight matrix W is generated according to both queen and rook criteria on regular $m \times m$ grids, leading to a sample size of $n = m^2$. While the queen specification states that two polygons are neighbors if they share a border or a vertex, the rook specification states that two polygons are neighbors if they share a border. The contiguity matrix is typically used as the spatial weight matrix for data represented by areal units

(polygons) that vary in size. Both weight matrices are row-normalized so that each row sums to unity. This study considers all combinations of the true parameters $\alpha_1 \in \{0.3, 0.5, 0.8\}$ and $\lambda \in \{0.1, 0.3, 0.5, 0.8, 1.0\}$, and the values of α_0 and σ^2 are set equal to 1.0 and 0.1. Note that the parameter space of α_1 is specified such that $I - \alpha_1 W$ is nonsingular, which requires that $\alpha_1 \in (\omega_{\min}^{-1}, \omega_{\max}^{-1})$ where $\omega_{\min}$ and $\omega_{\max}$, respectively, are the smallest (i.e. the most negative) and the largest real eigenvalues of W. For each combination of α_1 and λ, this procedure is repeated 1,000 times using samples of size $n = 100, 400$, and 900. Following Kelejian and Prucha (1999), the quality of an estimate is evaluated in terms of its bias and the root mean squared error (RMSE). The measure of bias is defined as the average difference between the estimator and the true value, while the RMSE is defined as the square root of the sum of the variance and the squared bias of the estimator.

4.2 Simulation Results

The simulation results using the queen contiguity are reported in Table 1, and those using the rook contiguity matrix are reported in Table 2. In each table, the first two columns are true values of the parameters of interest, α_1 and λ, and the remaining columns present the estimated bias and the RMSE of the two parameters for various combinations of sample size n and parameter values α_1 and λ.

First consider the simulation results based on the queen contiguity matrix reported in Table 1. As a general observation it seems that, on average, the bias of α_1 does not follow any particular pattern with respect to the parameter set of high or low values of α_1 and λ. Nonetheless, for a large true value of α_1, $\alpha_1 = 0.8$ here, the estimator of α_1 displays small bias, and the average RMSE is the lowest across all values of λ. Especially for $\alpha_1 = 0.8$ and $\lambda = 0.1$, the estimator of α_1 exhibits the lowest RMSE. Comparing the results associated with each value of λ across all sample sizes, it is found that increasing the sample size improves the quality of the estimates, i.e. the bias and RMSE become uniformly smaller with larger samples.

Another important parameter of interest is λ, which is the transformation parameter in the BC-SARCH model. It is shown that the estimator performs reasonably well in estimating λ in terms of bias and RMSE. In general, for small true values of λ, the estimator tends to produce better estimates with small bias and RMSE. In particular, the estimator with $\lambda = 0.1$ has the smallest RMSE across all values of α_1 and sample sizes, while the largest bias corresponds to a situation where the model is a linear form ($\lambda = 1$). The RMSE is shown to decrease as the sample size increases. The simulation results using the rook contiguity matrix reported in Table 2 are in line with the findings from the results reported in Table 1, suggesting that the performances of the estimators are robust to spatial weight matrix specifications.

TABLE 1 Bias and RMSE for estimators of α_1 and λ based on queen contiguity

		$n = 100$				$n = 400$				$n = 900$			
		α_1		λ		α_1		λ		α_1		λ	
		Bias	RMSE	Bias	RMSE	Bias	RMSE	Bias	RMSE	Bias	RMSE	Bias	RMSE
$\alpha_1 = 0.1$	$\lambda = 0.1$	-0.039	0.165	0.074	0.215	-0.013	0.089	0.023	0.114	-0.009	0.061	0.012	0.087
	$\lambda = 0.3$	-0.049	0.180	0.037	0.284	-0.015	0.093	-0.005	0.164	-0.008	0.061	0.001	0.114
	$\lambda = 0.5$	-0.055	0.189	-0.009	0.319	-0.011	0.094	-0.004	0.198	-0.006	0.063	-0.004	0.130
	$\lambda = 0.8$	-0.051	0.183	-0.100	0.335	-0.014	0.096	-0.047	0.217	-0.003	0.060	-0.010	0.146
	$\lambda = 1.0$	-0.056	0.191	-0.233	0.385	-0.017	0.092	-0.103	0.185	-0.006	0.061	-0.074	0.129
$\alpha_1 = 0.3$	$\lambda = 0.1$	-0.049	0.151	0.074	0.215	-0.013	0.080	0.019	0.115	-0.004	0.054	0.006	0.084
	$\lambda = 0.3$	-0.048	0.174	0.024	0.287	-0.019	0.088	0.010	0.175	-0.008	0.056	0.001	0.117
	$\lambda = 0.5$	-0.058	0.181	0.014	0.347	-0.013	0.083	0.010	0.207	-0.008	0.055	-0.001	0.142
	$\lambda = 0.8$	-0.050	0.168	-0.148	0.383	-0.012	0.086	-0.042	0.226	-0.007	0.056	-0.018	0.157
	$\lambda = 1.0$	-0.050	0.167	-0.246	0.405	-0.018	0.085	-0.129	0.223	-0.005	0.055	-0.089	0.153
$\alpha_1 = 0.5$	$\lambda = 0.1$	-0.040	0.126	0.065	0.201	-0.015	0.067	0.025	0.121	-0.009	0.045	0.008	0.084
	$\lambda = 0.3$	-0.054	0.145	0.034	0.291	-0.017	0.073	0.003	0.181	-0.006	0.044	-0.005	0.126
	$\lambda = 0.5$	-0.066	0.158	-0.016	0.349	-0.015	0.070	0.010	0.224	-0.010	0.048	0.003	0.156
	$\lambda = 0.8$	-0.069	0.160	-0.134	0.390	-0.015	0.071	-0.041	0.241	-0.006	0.049	-0.015	0.179
	$\lambda = 1.0$	-0.065	0.157	-0.273	0.446	-0.015	0.070	-0.136	0.236	-0.005	0.048	-0.093	0.162
$\alpha_1 = 0.8$	$\lambda = 0.1$	-0.041	0.084	0.023	0.135	-0.013	0.042	0.011	0.101	-0.006	0.028	0.004	0.076
	$\lambda = 0.3$	-0.046	0.101	-0.020	0.237	-0.016	0.044	0.003	0.186	-0.007	0.028	-0.005	0.141
	$\lambda = 0.5$	-0.050	0.101	-0.071	0.345	-0.013	0.044	-0.022	0.260	-0.004	0.027	0.000	0.194
	$\lambda = 0.8$	-0.051	0.102	-0.211	0.456	-0.013	0.042	-0.089	0.315	-0.007	0.028	-0.053	0.241
	$\lambda = 1.0$	-0.052	0.108	-0.343	0.534	-0.012	0.044	-0.211	0.360	-0.006	0.028	-0.147	0.257

Note: The spatial weight matrix is derived using queen contiguity. The values of α_0 and σ^2 are set equal to 1.0 and 0.1. Each set of simulation results is based on 1,000 Monte Carlo samples.

5 Empirical Analysis

5.1 Data

I base the empirical analysis on residential sales data obtained through the multiple listing service (MLS) used by Illinois REALTORS®.[6] The data include records of all residential property sales in the city of Chicago and cover the 10-year period running from 2009 through 2018. These properties are comprised of single-family properties and condominiums. To remove outliers, transactions that take place at extreme prices, below the first or above the ninety-ninth percentile of the distribution of raw prices, are excluded. The resulting dataset covers 258,017 transactions.

[6]The multiple listing service (MLS) is a private real estate listing service where real estate property information is listed and searched by participating members (e.g. real estate agents).

TABLE 2 Bias and RMSE for estimators of α_1 and λ based on rook contiguity

		$n = 100$				$n = 400$				$n = 900$			
		α_1		λ		α_1		λ		α_1		λ	
		Bias	RMSE	Bias	RMSE	Bias	RMSE	Bias	RMSE	Bias	RMSE	Bias	RMSE
$\alpha_1 = 0.1$	$\lambda = 0.1$	-0.016	0.124	0.071	0.213	-0.006	0.066	0.017	0.114	-0.001	0.045	0.009	0.082
	$\lambda = 0.3$	-0.023	0.128	0.020	0.275	-0.004	0.067	-0.005	0.163	-0.002	0.045	0.003	0.116
	$\lambda = 0.5$	-0.021	0.131	-0.005	0.332	-0.004	0.068	0.007	0.198	-0.001	0.048	-0.001	0.131
	$\lambda = 0.8$	-0.017	0.134	-0.106	0.347	-0.006	0.066	-0.015	0.203	-0.002	0.045	-0.012	0.150
	$\lambda = 1.0$	-0.028	0.135	-0.220	0.374	-0.005	0.068	-0.105	0.190	-0.002	0.046	-0.085	0.142
$\alpha_1 = 0.3$	$\lambda = 0.1$	-0.028	0.118	0.069	0.209	-0.007	0.062	0.017	0.117	-0.003	0.043	0.008	0.080
	$\lambda = 0.3$	-0.027	0.127	0.028	0.285	-0.007	0.067	0.008	0.171	-0.002	0.043	-0.002	0.118
	$\lambda = 0.5$	-0.028	0.126	-0.006	0.339	-0.005	0.064	-0.011	0.203	-0.003	0.045	-0.007	0.138
	$\lambda = 0.8$	-0.027	0.131	-0.099	0.351	-0.009	0.064	-0.032	0.215	-0.004	0.042	-0.018	0.157
	$\lambda = 1.0$	-0.025	0.121	-0.225	0.391	-0.012	0.064	-0.112	0.205	-0.003	0.042	-0.081	0.145
$\alpha_1 = 0.5$	$\lambda = 0.1$	-0.027	0.100	0.055	0.189	-0.008	0.055	0.019	0.109	-0.005	0.038	0.011	0.081
	$\lambda = 0.3$	-0.035	0.116	0.024	0.281	-0.012	0.058	-0.002	0.167	-0.004	0.038	0.001	0.116
	$\lambda = 0.5$	-0.032	0.112	-0.015	0.348	-0.009	0.057	-0.006	0.213	-0.003	0.037	-0.001	0.147
	$\lambda = 0.8$	-0.038	0.115	-0.141	0.391	-0.009	0.057	-0.053	0.234	-0.003	0.037	-0.009	0.162
	$\lambda = 1.0$	-0.038	0.123	-0.280	0.453	-0.008	0.056	-0.129	0.234	-0.005	0.038	-0.084	0.148
$\alpha_1 = 0.8$	$\lambda = 0.1$	-0.029	0.070	0.027	0.135	-0.010	0.035	0.007	0.093	-0.005	0.024	0.004	0.071
	$\lambda = 0.3$	-0.034	0.084	-0.011	0.238	-0.009	0.034	0.002	0.168	-0.004	0.023	-0.009	0.125
	$\lambda = 0.5$	-0.032	0.076	-0.055	0.343	-0.009	0.036	-0.001	0.239	-0.004	0.023	-0.011	0.173
	$\lambda = 0.8$	-0.033	0.077	-0.176	0.429	-0.010	0.036	-0.068	0.283	-0.005	0.023	-0.036	0.217
	$\lambda = 1.0$	-0.037	0.081	-0.290	0.477	-0.008	0.035	-0.191	0.333	-0.004	0.023	-0.119	0.212

Note: The spatial weight matrix is derived using rook contiguity. The values of α_0 and σ^2 are set equal to 1.0 and 0.1. Each set of simulation results is based on 1,000 Monte Carlo samples.

Several factors are considered in selecting appropriate spatial units to enable the study to represent neighborhoods. These include homogeneity in terms of socioeconomic status within the spatial unit; large enough population size to minimize the problem of small numbers; data availability; acceptability by urban planners and policy-makers; and the stability of the boundaries over time for future analyses. Based on these criteria, census tracts are chosen as the spatial units for the analysis, owing mainly to their homogeneity with respect to socioeconomic and demographic characteristics.[7] Furthermore, most census data are reported at this level of geography and the boundaries of the census tracts follow permanent and easily recognizable physical features.

There are 801 census tracts in Chicago and, for ease of interpretation, 77 community areas are used as references for the neighborhoods.[8] A detailed description of the areas can be found in Table 13 in the Appendix.

[7] Census tracts are small, relatively stable spatial units with population ranging between 2,500 and 8,000 with an average of approximately 4,000, and are designed to be homogeneous with respect to population characteristics, economic status, and living conditions.

[8] The community areas are well-defined, stable geographical regions designated by the Social Science Research Committee at the University of Chicago and officially recognized by the city of Chicago.

Figure 3 shows a map of Chicago with the 801 census tracts outlined in light blue and the 77 community areas outlined in solid black. It should be noted, however, that several tracts in which there are no observed transactions are eliminated from the analysis, leading to reduced and varying sample sizes across years (see Table 3).

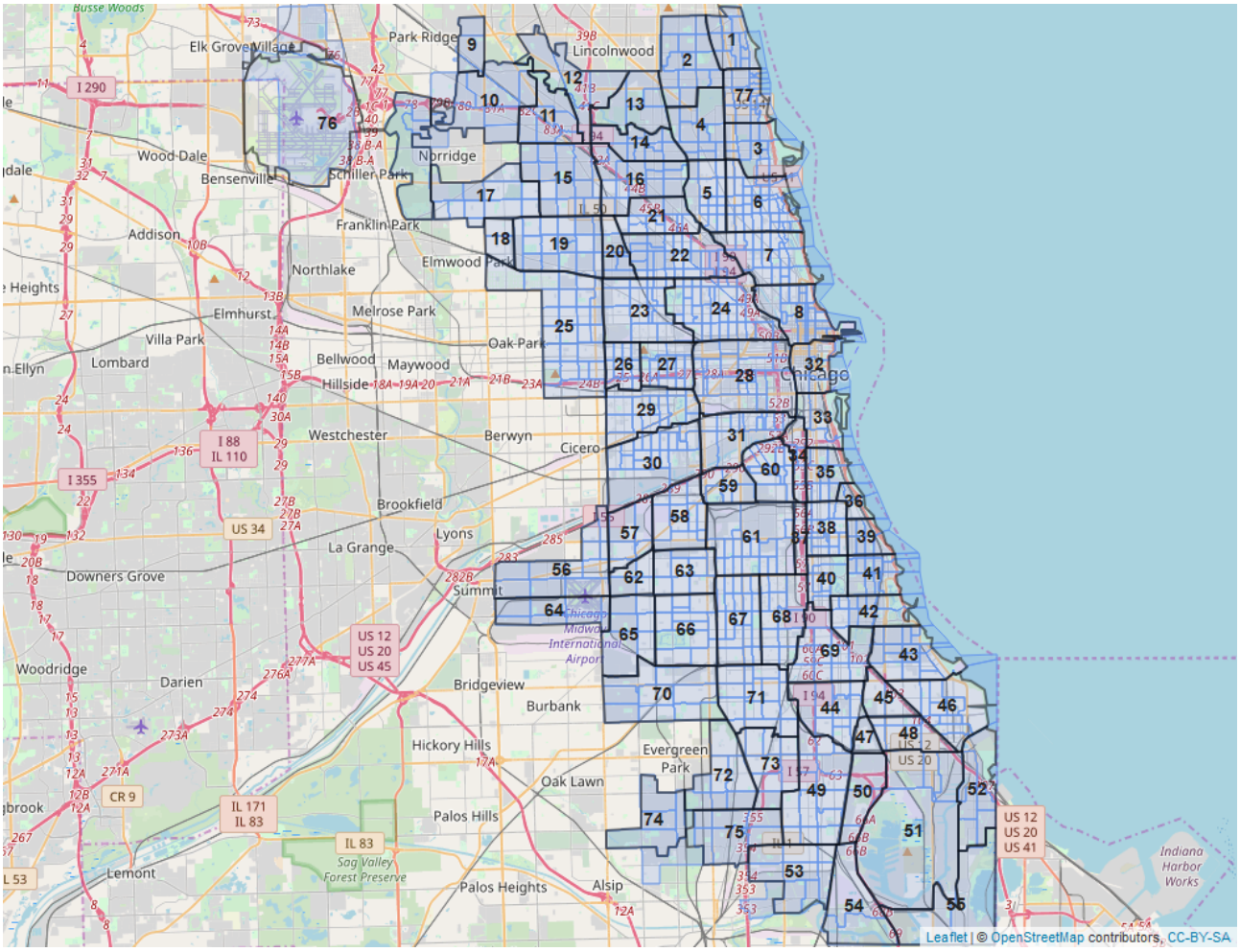

FIGURE 3 Chicago community areas with census tracts

Data Source: U.S. Census Bureau, OpenStreetMap.
Note: The listed numbers refer to the codes for Chicago community areas (see Table 13 in the Appendix for details).

All transaction records within the study area are geocoded using ArcGIS 10.6 and aggregated to the census-tract level to calculate an annual median price for each tract. The rationale for using median home prices in this study is its long history and extensive coverage of census tracts. It has been frequently argued that the repeat sales method is a considerable improvement over median sales prices as it controls for price appreciation that arises from significant positive or negative changes in property quality.[9] The repeat sales measure suffers a serious loss in the number of observations available to estimate the index, however, as it excludes properties

[9]The repeat sales approach assumes that the quality attributes and their coefficients for each house are constant between two sales dates. The S&P/Case-Shiller and the Federal Housing Finance Agency (FHFA) indices are based on repeat sales, while the National Association of Realtors (NAR) report the median prices of all houses that have sold (Bailey et al., 1963; Case and Shiller, 1987).

for which there is only one price observation, and it is not clear that properties that have sold more than once are representative of the overall housing market (McMillen, 2012). Clapp et al. (1991) also point out that the repeat sales measure may suffer from added noise when compared with price indices that are constructed using all transactions. In spite of all these shortcomings, however, the most widely used home price measures in government reports are based on the repeat sales method, including the ubiquitous S&P/Case-Shiller and the Federal Housing Finance Agency (FHFA) price indices. Such data have recently become available at the census-tract level by the FHFA (Bogin et al., 2019), but as expected they use a very limited number of census tracts, excluding a large portion of residential sales data.

Nevertheless, upon close inspection of the FHFA repeat sales price index and the calculated median price index for this study, it is found that the two price series exhibit similar overall patterns across census tracts for all years, with the average correlation coefficient equaling approximately 0.5 ($p < 0.001$). This result indicates that there will not be a large difference between the empirical results derived from the two data series and that the median price may reflect regional housing prices reasonably well with its robustness to selection and exclusion criteria. Also, the repeat sales index measures only relative prices within a census tract over time but not across tracts. Because this study focuses on cross-sectional variation in housing price volatility using the absolute dollar value of housing, repeat sales data are not well suited for this purpose. Capozza et al. (2004) and Cannon et al. (2006) also use median price data for their cross-sectional analysis across the U.S. housing market. In particular, Cannon et al. (2006) use annual data on median ZIP code home prices to study the cross-sectional role of volatility, price level, stock market risk, and idiosyncratic volatility in housing returns. More sophisticated measures of the housing price index are possible, e.g. the hedonic price index, but they are beyond the scope of this research.[10]

Therefore, this study relies on the median price index and the calculated median prices are used to construct the key variable of interest in this study, housing returns. The return series is obtained from the first difference of log annual median house prices, i.e. $y_{i,t} = \log\left(P_{i,t}/P_{i,t-1}\right)$, where at census tract (location) i, $P_{i,t}$ and $P_{i,t-1}$ are the median prices at time t and $t-1$, respectively.[11] It should be noted that following Willcocks (2010), the returns are not smoothed or adjusted for inflation as adjustment could hide the impact of volatility changes between adjacent time periods.

To investigate the spatial dependence structure in volatility, the series of squared returns y_i^2 and log-squared

[10] The hedonic price index combines data on sales price with property and location characteristics, and controls for factors that might affect the sales price of a house.

[11] Hayunga et al. (2019) argue that homeowner characteristics influence their maintenance and home-improvement behaviors, which in turn affect home values and thus the observed pecuniary return. This analysis requires mortgage information data at initial purchase, which are not available from the MLS records; the current study thus treats observed housing returns as actual returns despite the possibility of overstatement.

returns $\log y_i^2$ are considered as proxies of the volatility measures, which are the linear and log-linear cases nested within the BC-SARCH model. The logarithm of squared returns is problematic when the returns are zero or very small in magnitude. To avoid the problem of taking the logarithm of zero, Fuller (1996) proposes a slight modification of the squared returns, which is given by

$$\log \tilde{y}_i^2 = \log(y_i^2 + \gamma s^2) - \frac{\gamma s^2}{y_i^2 + \gamma s^2}, \tag{15}$$

where s^2 is the sample variance of returns and γ is a small constant, with γ set equal to 0.02, following Fuller (1996). This modified version will, for convenience, be hereinafter referred to as the log-squared returns. Table 3 presents summary statistics for the returns and two volatility series, squared returns and log-squared returns, including the Jarque-Bera test statistics for normality for each year during the study period running from 2009 through 2018.

TABLE 3 Descriptive statistics

	Returns					Squared returns					Log-squared returns				
	Mean	S.D.	Skew.	Kurt.	J-B	Mean	S.D.	Skew.	Kurt.	J-B	Mean	S.D.	Skew.	Kurt.	J-B
2009	−0.37	0.51	−1.00	5.96	1258.8***	0.40	0.95	5.24	38.13	49713.9***	−2.66	2.06	0.03	−0.91	25.9***
2010	−0.06	0.45	−0.56	4.44	673.5***	0.21	0.53	4.83	27.98	28125.3***	−3.48	2.03	0.28	−0.83	31.4***
2011	−0.09	0.46	0.43	5.23	905.0***	0.22	0.56	5.37	34.85	42695.5***	−3.19	1.92	0.10	−0.71	17.2***
2012	−0.02	0.38	−0.24	4.01	521.6***	0.14	0.35	7.50	90.41	267722.8***	−3.50	1.89	0.06	−0.82	21.6***
2013	0.11	0.38	−0.13	3.29	350.8***	0.16	0.35	4.81	32.59	36914.0***	−3.38	1.92	−0.03	−0.75	17.9***
2014	0.14	0.37	0.05	6.67	1434.5***	0.15	0.41	7.44	81.27	219901.5***	−3.58	1.99	0.04	−0.84	22.5***
2015	0.11	0.38	0.61	4.53	716.6***	0.16	0.40	5.69	47.62	77926.1***	−3.78	2.10	0.24	−0.96	36.7***
2016	0.10	0.37	0.03	3.34	360.6***	0.15	0.33	4.78	29.59	31026.9***	−3.59	2.00	0.07	−0.97	30.3***
2017	0.12	0.35	0.50	3.81	497.9***	0.14	0.32	4.50	24.85	22386.8***	−3.79	2.02	0.18	−0.87	28.2***
2018	0.10	0.33	0.63	4.10	592.6***	0.12	0.29	6.12	56.31	106695.4***	−3.90	2.02	0.17	−0.93	31.1***

Note: This table describes several summary statistics, including means (%), standard deviations (S.D., %), skewness (Skew.), kurtosis (Kurt.) and the J–B (Jarque–Bera) test statistics. Under the null hypothesis for normality, the J-B statistic is distributed as $\chi^2(2)$. *** $p < 0.01$; ** $p < 0.05$; * $p < 0.1$

The figures reported in columns 1-5 indicate that the Chicago housing market experienced negative annual returns over the period during which the market falls (2009-2012) while returns increase when the market rises (2013-2018). In particular, the lowest annual return is observed in 2009 in the aftermath of the recent crisis. Furthermore, during the overall period, most of the return series display only small variations from zero skewness, although they exhibit excess kurtosis. Finally, the Jarque-Bera test indicates that the returns are not normally distributed for the overall period. The remaining columns present summary statistics for the two volatility measures: squared returns and log-squared returns. The descriptive statistics for the squared-return

series clearly indicates a positively skewed and leptokurtic distribution. The Jarque-Bera test further confirms a serious departure from normality. On the other hand, the logarithmic transform renders the squared returns approximately normal as the values of the Jarque-Bera test for the log-squared returns are considerably lower than the corresponding values for the returns and the squared returns.

5.2 Preliminary Tests

To understand whether the three return series reflect spatial dependence, a global Moran's I test for spatial patterns is undertaken for cross-sectional data from 2009 through 2018 separately. The Moran's I is a widely used test for the presence of spatial dependence, and in this study the queen and rook contiguity weight matrices are considered to check the robustness of the test results. Table 4 provides the test results in which the results reported in Panel A are based on the queen contiguity matrix, and those reported in Panel B are based on the rook contiguity matrix.

The results are in line with expectations presented visually in the introduction and are not sensitive to the choice of the spatial weight matrix. Both measures of volatility exhibit a high degree of spatial dependence, while there is no or only weak statistical evidence for spatial dependence in the returns, with the exception for 2009, when the effects of the financial crisis led to significant negative returns for most tracts, which can be identified in Panel (a) of Figure 4.[12]

On the whole, the above results appear to be analogous to the well-known stylized fact in the time-series literature that, in contrast to the lack of serial dependence in returns, the autocorrelation for the squared returns is always positive and significant. Note that, in the case of log-squared returns, the reported test statistics are generally larger and p-values are lower (more significant). The presence of spatial dependence in the return series indicates that the housing market is spatially inefficient, and therefor the housing returns could contain useful information for predicting the returns in neighboring locations. This result is not surprising because the unique features of a housing market, such as transaction costs, infrequent transactions, and a high degree of heterogeneity, may limit arbitrage opportunities, leading to pricing inefficiencies (Case and Shiller, 1988).

5.3 Cross-Sectional Estimation Results

The BC-SARCH model specified in equation (1) is estimated separately for each of the ten years beginning in 2009, and the cross-section results are presented in Table 5, where the parameters are estimated by the maximum likelihood method. After estimating the coefficients, their corresponding standard errors are obtained from the

[12] In the finance literature, several papers have documented that an autocorrelation of stock returns exists, particularly during the post-crisis period (Islam et al., 2007; Sarwar and Khan, 2017).

TABLE 4 Moran's I tests

	Returns		Squared returns		Log-squared returns	
	Moran's I	p-value	Moran's I	p-value	Moran's I	p-value
Panel A: Queen contiguity						
2009	0.247***	8×10^{-33}	0.251***	2×10^{-35}	0.406***	2×10^{-84}
2010	0.078***	6×10^{-5}	0.139***	3×10^{-12}	0.191***	1×10^{-20}
2011	0.062***	1×10^{-3}	0.079***	4×10^{-5}	0.161***	3×10^{-15}
2012	0.058***	2×10^{-3}	0.074***	6×10^{-5}	0.208***	5×10^{-24}
2013	−0.015	0.739	0.080***	3×10^{-5}	0.128***	2×10^{-10}
2014	0.016	0.197	0.069***	2×10^{-4}	0.151***	8×10^{-14}
2015	0.023	0.113	0.193***	3×10^{-23}	0.231***	4×10^{-30}
2016	0.020	0.146	0.247***	9×10^{-35}	0.300***	2×10^{-48}
2017	0.050***	7×10^{-3}	0.228***	1×10^{-29}	0.287***	2×10^{-44}
2018	0.094***	2×10^{-6}	0.183***	8×10^{-21}	0.270***	1×10^{-39}
Panel B: Rook contiguity						
2009	0.267***	7×10^{-28}	0.249***	2×10^{-25}	0.425***	2×10^{-66}
2010	0.086***	2×10^{-4}	0.140***	2×10^{-9}	0.188***	5×10^{-15}
2011	0.060***	6×10^{-3}	0.078***	4×10^{-4}	0.168***	2×10^{-12}
2012	0.063***	4×10^{-3}	0.082***	1×10^{-4}	0.211***	3×10^{-18}
2013	−0.022	0.798	0.065***	3×10^{-3}	0.127***	7×10^{-8}
2014	0.014	0.258	0.046**	0.019	0.148***	4×10^{-10}
2015	0.009	0.333	0.201***	2×10^{-18}	0.247***	3×10^{-25}
2016	0.037*	0.056	0.266***	1×10^{-29}	0.294***	3×10^{-34}
2017	0.048**	0.022	0.258***	1×10^{-27}	0.298***	7×10^{-35}
2018	0.087***	1×10^{-4}	0.149***	7×10^{-11}	0.268***	1×10^{-28}

Note: For Panel A, the spatial weight matrix is based on queen contiguity. For Panel B, the spatial weight matrix is based on rook contiguity. $^{***}\ p < 0.01$; $^{**}\ p < 0.05$; $^{*}\ p < 0.1$

diagonal elements of the inverted Hessian matrix and used to perform a t-test for the null hypotheses that each of α_0, α_1, σ, and λ is equal to zero. The upper panel (Panel A) of Table 5 reports the estimation results using the queen contiguity matrix, and the results using the rook contiguity matrix are shown in the lower panel (Panel B).

The most noticeable result reported in Table 5 is that, as expected, there is strong and significant spatial dependence in Box-Cox transformed squared returns in all years, with coefficient values ranging from 0.293 for 2013 to 0.613 for 2009. This result provides strong evidence for the presence of spatial clustering in volatility discussed earlier in connection with Figure 1 and Table 4. That is, locations with high volatility tend to have neighbors with high volatility and those with low volatility tend to have neighbors with low volatility. The comparison of Panel A and Panel B reveals that such a result can be obtained with the rook contiguity matrix, although the rook contiguity matrix captures slightly less spatial dependence than the queen contiguity matrix because it considers fewer neighbors than the queen case.

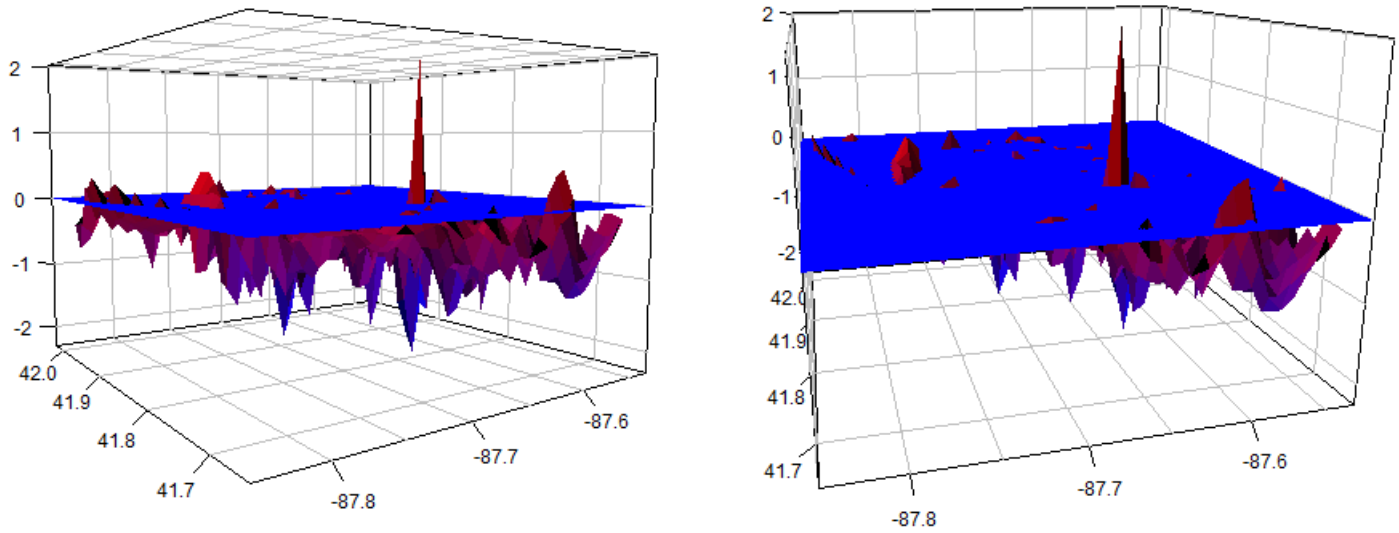

(a) Returns

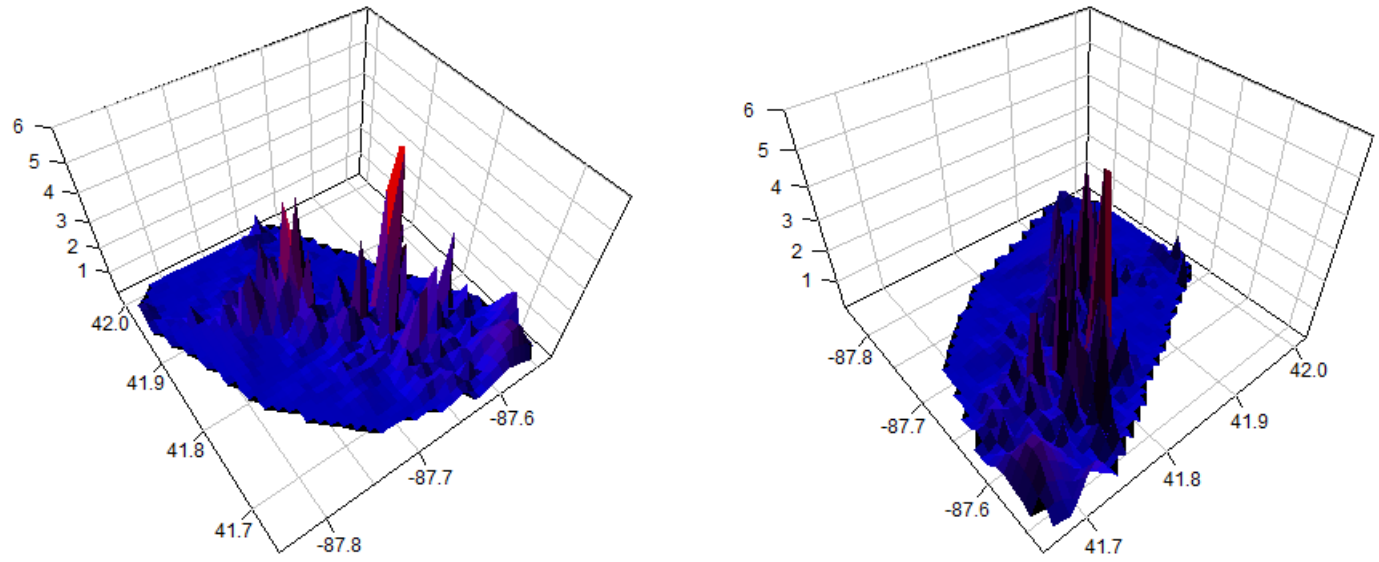

(b) Squared returns

FIGURE 4 Spatial distribution of returns and squared returns, 2009

TABLE 5 BC-SARCH model ML estimation results

	2009	2010	2011	2012	2013	2014	2015	2016	2017	2018
Panel A: Queen contiguity										
α_0	−0.837***	−1.901***	−1.782***	−1.708***	−1.870***	−1.997***	−1.815***	−1.365***	−1.604***	−1.639***
	(0.111)	(0.195)	(0.169)	(0.176)	(0.187)	(0.194)	(0.220)	(0.160)	(0.232)	(0.229)
α_1	0.613***	0.367***	0.338***	0.411***	0.293***	0.314***	0.434***	0.517***	0.471***	0.488***
	(0.031)	(0.040)	(0.041)	(0.038)	(0.040)	(0.038)	(0.039)	(0.032)	(0.039)	(0.039)
σ	2.021***	2.922***	2.375***	2.025***	1.898***	2.270***	2.778***	1.836***	2.006***	2.112***
	(0.008)	(0.010)	(0.010)	(0.012)	(0.010)	(0.012)	(0.013)	(0.011)	(0.015)	(0.016)
λ	0.118	0.094	0.106	0.101	0.132	0.112	0.095	0.120	0.113	0.101
	(0.214)	(0.431)	(0.313)	(0.323)	(0.316)	(0.406)	(0.558)	(0.320)	(0.504)	(0.525)
n	759	766	766	761	763	769	776	766	765	767
Log-likelihood	560.3	1163.7	938.5	1174.0	1072.6	1227.2	1416.8	1267.7	1399.6	1486.6
Pseudo R^2	0.221	0.070	0.039	0.050	0.041	0.037	0.108	0.160	0.160	0.117
Moran's I	−0.046	−0.017	−0.012	−0.018	−0.010	−0.018	−0.024	−0.035	−0.034	−0.021
(p-value)	(0.983)	(0.774)	(0.700)	(0.791)	(0.656)	(0.788)	(0.872)	(0.947)	(0.944)	(0.829)
J-B	8.052	2.601	0.405	0.800	0.591	1.193	5.509	3.679	1.880	3.792
(p-value)	(0.018)	(0.272)	(0.817)	(0.670)	(0.744)	(0.551)	(0.064)	(0.159)	(0.391)	(0.150)
Panel B: Rook contiguity										
α_0	−0.901***	−2.123***	−1.927***	−1.889***	−2.030***	−2.200***	−1.954***	−1.607***	−1.792***	−1.925***
	(0.109)	(0.186)	(0.157)	(0.170)	(0.176)	(0.189)	(0.207)	(0.159)	(0.224)	(0.222)
α_1	0.580***	0.296***	0.287***	0.352***	0.235***	0.246***	0.395***	0.437***	0.413***	0.405***
	(0.030)	(0.036)	(0.037)	(0.035)	(0.036)	(0.034)	(0.036)	(0.031)	(0.036)	(0.036)
σ	1.984***	3.000***	2.422***	2.077***	1.944***	2.314***	2.833***	1.962***	2.077***	2.267***
	(0.008)	(0.010)	(0.010)	(0.012)	(0.010)	(0.012)	(0.013)	(0.011)	(0.015)	(0.015)
λ	0.120	0.093	0.105	0.099	0.130	0.111	0.092	0.117	0.111	0.096
	(0.212)	(0.434)	(0.316)	(0.329)	(0.317)	(0.418)	(0.546)	(0.340)	(0.495)	(0.528)
n	759	766	766	761	763	769	776	766	765	767
Log-likelihood	558.7	1157.7	936.0	1169.0	1069.4	1222.5	1416.1	1255.4	1394.4	1476.0
Pseudo R^2	0.197	0.062	0.033	0.050	0.033	0.025	0.100	0.140	0.157	0.085
Moran's I	−0.044	−0.021	−0.016	−0.019	−0.009	−0.019	−0.024	−0.045	−0.040	−0.033
(p-value)	(0.957)	(0.786)	(0.724)	(0.762)	(0.618)	(0.761)	(0.826)	(0.963)	(0.942)	(0.901)
J-B	5.479	2.153	0.195	0.774	0.589	1.112	5.477	3.187	1.815	2.592
(p-value)	(0.065)	(0.341)	(0.907)	(0.679)	(0.745)	(0.573)	(0.065)	(0.203)	(0.404)	(0.274)

Note: For $H_0 : \lambda = 1$, the null is rejected in all cases. Standard errors appear in parentheses. Pseudo R^2 is computed as the squared correlation between the observed and predicted values of the dependent variable (Anselin, 1988). Diagnostic tests, including Moran's I test and the J-B (Jarque–Bera) test, are implemented to examine the spatial dependence and normality of the residuals. *** $p < 0.01$; ** $p < 0.05$; * $p < 0.1$

Of particular interest is the transformation parameter λ. In every year, the estimated coefficients appear to be very close to zero, ranging from 0.094 for 2010 to 0.132 for 2013. The *t*-test indicates that the null hypothesis that $\lambda = 0$ is not rejected and thus λ is not significantly different from zero, pointing to a log-linear form as the best fit. If the test is based on the null hypothesis that $\lambda = 1$, the null hypothesis is clearly rejected for all years (results available from the author upon request). Therefore, the estimation results of the BC-SARCH model applied to the empirical data indicate that there is strong evidence against a linear model and in favor

of a log-linear model with $\lambda \to 0$. A further implication of the estimated λ concerns the CES-type volatility production function presented in equation (6) in Section 3, where λ is viewed as the substitution parameter and is used to derive the elasticity of substitution $\eta = \frac{1}{1-\lambda}$. The estimated values of λ close to 0 suggest values of η close to 1 across the study period. Recalling that the zero value of λ and the value of the unity of η imply that the production function takes the Cobb-Douglas form where autonomous variance and neighborhood-induced variance are two inputs, it can be concluded that the neighborhood-induced variance is as important as the autonomous variance in aggregate variance.

Finally, at the bottoms of each panel in Table 5, several model-specification tests are performed to verify the validity of the estimated BC-SARCH model using Moran's *I* test and the Jarque-Bera normality test for the residuals. The Moran's *I* test of the residuals fails to reject the null hypothesis of the absence of spatial dependence, thus suggesting that the spatial dependence has been entirely captured by the model and is not left in the residuals. With regard to normality, the Jarque–Bera statistic confirms the normality behavior of the estimated residuals. The same conclusion can be drawn when both tests are replicated using the rook contiguity matrix, which further strengthens the usefulness of the BC-SARCH model.

All in all, the above results support that the presence of conditional volatility over space is non-trivial and the proposed BC-SARCH model is a powerful tool for modeling such spatially dependent heterogeneity. The results further reveal that a model of the log-linear form may provide an adequate representation of spatial volatility. From an economic perspective, the most well-known benefits of using a log-linear model is that it can not only approximate a normal distribution and reduce skewness but also make it easier to interpret the empirical results. While a Box-Cox transformation severely complicates the interpretation of the coefficients, the coefficients of a log-linear model lend themselves to straightforward interpretations such as elasticity, a measurement of the responsiveness of one variable to a change in another variable in percentage terms. Therefore, as discussed in Section 3, a log-linear model allows α_1 to be interpreted as *neighborhood elasticity*, which measures the percentage change in volatility of neighboring locations with respect to a one percent change in volatility in one location. Table 6 reports the estimation results of the final log-linear model in equation (4), which are obtained using the ML method. The results reveal that, despite the simplicity and convenience of the model, the main findings remain unaltered.

The estimated coefficients of the spatial dependence parameter α_1, i.e. neighborhood elasticity, are still positive and highly significant at the 1% significance level across all years with almost the same magnitudes as those obtained with the BC-SARCH model, suggesting an inherent volatility dependence among cross-sectional units. Values of the coefficients range from 0.296 for 2013 to 0.623 for 2019 with a cross-sectional average of 0.435 for the queen contiguity, while for the rook contiguity it varies between 0.240 for 2013 and 0.587 for 2009

TABLE 6 Log-linear model estimation results

	2009	2010	2011	2012	2013	2014	2015	2016	2017	2018
Panel A: Queen contiguity										
α_0	−0.990***	−2.155***	−2.101***	−2.039***	−2.363***	−2.438***	−2.079***	−1.698***	−1.890***	−1.937***
	(0.118)	(0.189)	(0.179)	(0.183)	(0.194)	(0.202)	(0.193)	(0.169)	(0.183)	(0.187)
α_1	0.623***	0.380***	0.344***	0.414***	0.296***	0.318***	0.449***	0.521***	0.499***	0.502***
	(0.038)	(0.050)	(0.052)	(0.049)	(0.054)	(0.053)	(0.048)	(0.044)	(0.045)	(0.045)
n	759	766	766	761	763	769	776	766	765	767
Log-likelihood	-1510.6	-1600.0	-1563.4	-1530.1	-1565.8	-1601.3	-1631.6	-1551.6	-1560.1	-1568.5
Pseudo R^2	0.343	0.112	0.088	0.133	0.063	0.075	0.157	0.224	0.206	0.202
Moran's I	−0.048	−0.019	−0.014	−0.019	−0.010	−0.019	−0.026	−0.036	−0.037	−0.022
(p-value)	(0.987)	(0.801)	(0.735)	(0.806)	(0.662)	(0.798)	(0.885)	(0.954)	(0.958)	(0.840)
J-B	8.273	22.672	14.573	17.413	16.360	18.642	24.657	20.713	14.837	18.736
(p-value)	(0.016)	(0.000)	(0.001)	(0.000)	(0.000)	(0.000)	(0.000)	(0.000)	(0.001)	(0.000)
Panel B: Rook contiguity										
α_0	−1.078***	−2.398***	−2.269***	−2.243***	−2.550***	−2.674***	−2.250***	−1.988***	−2.112***	−2.243***
	(0.113)	(0.178)	(0.167)	(0.173)	(0.179)	(0.188)	(0.182)	(0.167)	(0.176)	(0.182)
α_1	0.587***	0.311***	0.291***	0.357***	0.240***	0.253***	0.404***	0.439***	0.441***	0.424***
	(0.036)	(0.047)	(0.048)	(0.046)	(0.049)	(0.049)	(0.044)	(0.043)	(0.043)	(0.044)
n	759	766	766	761	763	769	776	766	765	767
Log-likelihood	-1513.4	-1606.1	-1566.2	-1535.1	-1568.9	-1605.7	-1633.7	-1564.8	-1566.2	-1579.2
Pseudo R^2	0.352	0.094	0.081	0.122	0.053	0.061	0.156	0.192	0.195	0.175
Moran's I	−0.047	−0.023	−0.017	−0.019	−0.009	−0.019	−0.027	−0.047	−0.045	−0.034
(p-value)	(0.968)	(0.810)	(0.743)	(0.766)	(0.626)	(0.770)	(0.856)	(0.970)	(0.963)	(0.912)
J-B	11.391	24.190	15.280	18.336	16.353	19.237	25.601	21.514	14.867	19.466
(p-value)	(0.003)	(0.000)	(0.000)	(0.000)	(0.000)	(0.000)	(0.000)	(0.000)	(0.001)	(0.000)

Note: Standard errors appear in parentheses. Pseudo R^2 is computed as the squared correlation between the observed and predicted values of the dependent variable (Anselin, 1988). Diagnostic tests, including Moran's I test and the J-B (Jarque–Bera) test, are implemented to examine the spatial dependence and normality of the residuals. $^{***}\ p < 0.01$; $^{**}\ p < 0.05$; $^{*}\ p < 0.1$

with a cross-sectional average of 0.375. This result suggests that, irrespective of the spatial weight matrix used, a 1% increase in volatility leads to an approximately 0.4% increase in volatility in neighboring locations.

Conducting the same diagnostic tests as I applied to the BC-SARCH model for the log-linear model reveals a similar regime. Moran's I test confirms that no evidence of remaining residual spatial dependence is found. Although the Jarque-Bera test rejects normality, the small values of the statistic imply that there is no severe departure from normality. In particular, when compared with the observed deviation from normality in the unconditional distribution of the squared returns presented in Table 3, the improvement in the normality of the residuals obtained by adopting the conditional log-linear model is substantial. To further examine how well the log-linear model identifies the spatially dependent pattern of volatility, the estimated squared returns obtained from the model for the year 2017 are plotted over the census tracts on the 3D maps with two views presented in Panels (a) and (b) of Figure 5, respectively corresponding to the queen contiguity and rook contiguity. As can

be seen, the spatial dependence pattern is well reproduced by the model for both weight matrices. While the lowest estimates of squared returns are distributed over the north-east side past downtown Chicago, the estimated squared returns show clear spikes on the west and south sides of the city, with distinct clusters. All in all, the simplified log-linear model appears to be an appropriate tool with which to describe the spatial dependence of volatility in the Chicago housing market.

Arguably, it might be worthwhile examining the possibility of applying the unchosen alternative, i.e. the linear model in equation (3), to identify the spatially dependent volatility pattern. The estimation results are reported in Table 7. As can be seen, the resulting estimates of α_1 consistently exhibit substantial and statistically significant spatial heteroskedasticity and volatility clustering across the cross-sectional units, even with the use of the simplest linear model. However, although the estimated coefficients remain statistically significant at the 1% significance level for every year, they are somewhat lower than those found in the log-linear model with greater variation over time. For extreme cases, the coefficient decreases from 0.344 to 0.190 for 2011, and from 0.414 to 0.204 for 2012. Nevertheless, the largest deviation from the log-linear model is detected in the diagnostic tests. Even though there is no remaining spatial dependence in the estimated residuals according to Moran's *I* test, the residuals severely depart from normality based on the Jarque-Bera test statistic and thus the statistical inference becomes increasingly less robust.

The fact that the log-linear model is far less misspecified than the linear model can also be illustrated by several test statistics based on the information matrix. As described by White (1982), information-matrix equality may be used as the basis for a test of model misspecification. Let $\mathbf{J}(\theta)$ denote the negative of the expectation of the Hessian and $\mathbf{K}(\theta)$ denote the expected outer product of the gradients for an unknown p-dimensional parameter vector θ. Then

$$\mathbf{J}(\theta) := -E\left[\frac{\partial^2 l(\theta)}{\partial\theta\partial\theta'}\right] \qquad \text{and} \qquad \mathbf{K}(\theta) := E\left[\frac{\partial l(\theta)}{\partial\theta}\left(\frac{\partial l(\theta)}{\partial\theta}\right)'\right], \tag{16}$$

where $l(\theta)$ is the log-likelihood function. White (1982) proposes the information matrix (IM) test, which exploits the fact that, under correct model specification, $\mathbf{J}(\theta_\mathbf{0}) = \mathbf{K}(\theta_\mathbf{0})$, which also implies $tr(\mathbf{J}(\theta_\mathbf{0}) - \mathbf{K}(\theta_\mathbf{0})) = 0$, where θ_0 denotes the true value of the parameter vector and $tr(A)$ is the trace of matrix A. The contrapositive statement implies that a difference between $\mathbf{J}(\theta_\mathbf{0})$ and $\mathbf{K}(\theta_\mathbf{0})$ indicates the presence of model misspecification. Thus if the information matrix equality is violated (i.e. $\mathbf{J}(\theta_\mathbf{0}) \neq \mathbf{K}(\theta_\mathbf{0})$), this is evidence against the model.

In contrast to the IM test, which relies on the difference between $\mathbf{J}(\theta_\mathbf{0})$ and $\mathbf{K}(\theta_\mathbf{0})$, Presnell and Boos (2004) propose an alternative test — the in-and-out-of-sample (IOS) test based on the information-matrix ratio. Let $y_i, ..., y_n$ denote independent random vectors with hypothesized densities or probability mass functions $f(y, \theta)$,

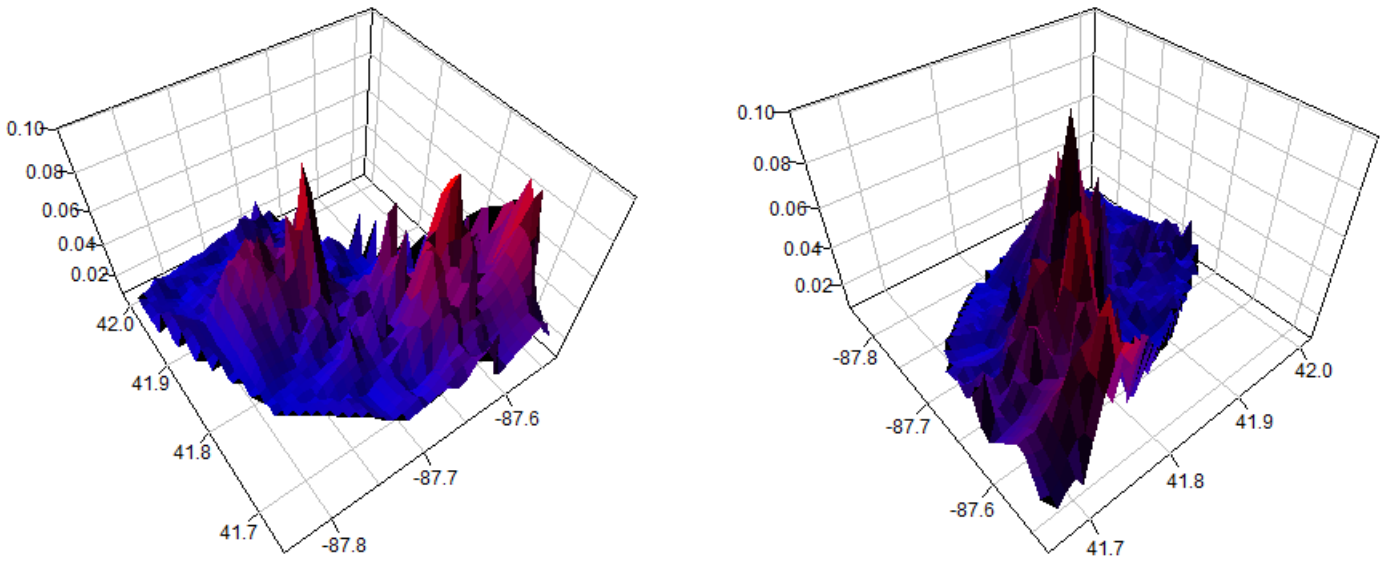

(a) Queen contiguity

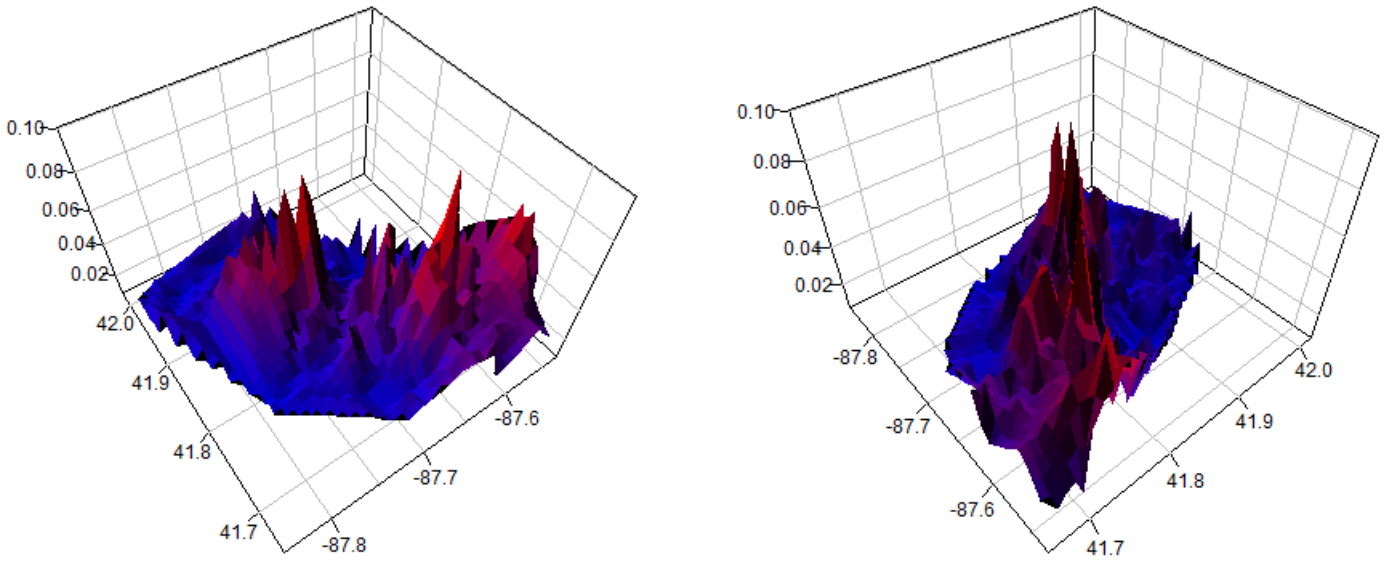

(b) Rook contiguity

FIGURE 5 Estimated squared returns, 2017

TABLE 7 Linear model estimation results

	2009	2010	2011	2012	2013	2014	2015	2016	2017	2018
Panel A: Queen contiguity										
α_0	0.213***	0.139***	0.176***	0.116***	0.129***	0.127***	0.095***	0.076***	0.073***	0.073***
	(0.037)	(0.021)	(0.024)	(0.015)	(0.015)	(0.017)	(0.016)	(0.013)	(0.012)	(0.012)
α_1	0.490***	0.328***	0.190***	0.204***	0.207***	0.181***	0.411***	0.503***	0.473***	0.395***
	(0.045)	(0.053)	(0.058)	(0.057)	(0.057)	(0.058)	(0.049)	(0.045)	(0.046)	(0.050)
n	759	766	766	761	763	769	776	766	765	767
Log-likelihood	-985.9	-580.7	-635.7	-285.1	-266.5	-397.1	-357.4	-184.0	-168.9	-116.8
Pseudo R^2	0.190	0.078	0.025	0.028	0.029	0.022	0.126	0.195	0.172	0.117
Moran's I	−0.027	−0.004	−0.005	−0.003	−0.005	−0.005	−0.020	−0.016	−0.018	−0.015
(p-value)	(0.901)	(0.556)	(0.571)	(0.536)	(0.570)	(0.581)	(0.828)	(0.761)	(0.789)	(0.757)
J-B	74821.9	27748.2	44022.3	290091.6	39377.9	229872.0	72626.3	25940.6	21822.0	130526.8
(p-value)	(0.000)	(0.000)	(0.000)	(0.000)	(0.000)	(0.000)	(0.000)	(0.000)	(0.000)	(0.000)
Panel B: Rook contiguity										
α_0	0.243***	0.153***	0.185***	0.120***	0.140***	0.139***	0.102***	0.084***	0.079***	0.089***
	(0.037)	(0.021)	(0.023)	(0.015)	(0.015)	(0.017)	(0.015)	(0.013)	(0.012)	(0.012)
α_1	0.415***	0.258***	0.152***	0.177***	0.134***	0.099*	0.361***	0.453***	0.428***	0.259***
	(0.044)	(0.049)	(0.051)	(0.051)	(0.051)	(0.052)	(0.046)	(0.043)	(0.044)	(0.049)
n	759	766	766	761	763	769	776	766	765	767
log-likelihood	-995.4	-584.7	-637.0	-285.3	-269.6	-400.2	-360.6	-186.2	-168.3	-131.1
Pseudo R^2	0.167	0.062	0.021	0.029	0.016	0.009	0.122	0.195	0.175	0.063
Moran's I	−0.032	−0.008	−0.005	−0.001	−0.005	−0.003	−0.008	−0.023	−0.030	−0.025
(p-value)	(0.896)	(0.607)	(0.553)	(0.488)	(0.556)	(0.525)	(0.618)	(0.819)	(0.886)	(0.848)
J-B	70293.5	27613.0	43351.8	287672.1	38115.9	225203.8	77533.1	21614.9	20132.4	126366.3
(p-value)	(0.000)	(0.000)	(0.000)	(0.000)	(0.000)	(0.000)	(0.000)	(0.000)	(0.000)	(0.000)

Note: Standard errors appear in parentheses. Pseudo R^2 is computed as the squared correlation between the observed and predicted values of the dependent variable (Anselin, 1988). Diagnostic tests including Moran's I test and the J-B (Jarque–Bera) test are implemented to examine the spatial dependence and normality of the residuals. $^{***}\ p < 0.01$; $^{**}\ p < 0.05$; $^{*}\ p < 0.1$

where θ is an unknown p-dimensional parameter. Let $\hat{\theta}$ be the maximum likelihood estimator of θ, and $\hat{\theta}_{(i)}$ be the MLE when the i-th observation is deleted from the entire sample. Presnell and Boos (2004) suggest that the single likelihood $f(y_i, \hat{\theta}_{(i)})$ can be regarded as the predictive likelihood by the other observations. Their proposed test statistic is the logarithm of the IOS likelihood ratio:

$$\text{IOS} = \log\left(\frac{\prod_{i=1}^{n} f(y_i, \hat{\theta})}{\prod_{i=1}^{n} f(y_i, \hat{\theta}_{(i)})}\right) = \sum_{i=1}^{n}\left[\log f(y_i, \hat{\theta}) - \log f(y_i, \hat{\theta}_{(i)})\right], \tag{17}$$

and its asymptotic form is

$$\text{IOS}_A = tr\big(-\hat{\mathbf{J}}^{-1}(\hat{\theta})\hat{\mathbf{K}}(\hat{\theta})\big) \tag{18}$$

and $\text{IOS} - \text{IOS}_A = o_p(n^{-1/2})$. Like the IM test, IOS_A also compares the two information matrices, but in

a ratio form instead of a subtractive form. If the model is correctly specified, it is expected that $\text{IOS}_A \xrightarrow{p} tr\big(\mathbf{J}(\theta_\mathbf{0})^{-1}\mathbf{K}(\theta_\mathbf{0})\big) = p$, the trace of the p-dimensional identity matrix. Under model misspecification, the two forms of the information generally differ, in which case IOS_A is expected to differ systematically from p.[13]

The two trace-based test statistics are used to statistically detect the model missipecification: the one under the null hypothesis that $tr\big(\mathbf{J}(\theta_\mathbf{0}) - \mathbf{K}(\theta_\mathbf{0})\big) = 0$ (Trace IM test) and the other under the null hypothesis that $tr\big(\mathbf{J}(\theta_\mathbf{0})^{-1}\mathbf{K}(\theta_\mathbf{0})\big) = p$, i.e. $tr\big(\mathbf{J}(\theta_\mathbf{0})^{-1}\mathbf{K}(\theta_\mathbf{0})\big) - p = 0$ (IOS_A test). Both $\mathbf{J}(\theta)$ and $\mathbf{K}(\theta)$ are derived in the Appendix. The resulting statistics are reported in Table 8 for both the linear and log-linear specifications, where, as before, I report the results using the queen contiguity in Panel A and I report the results using the rook contiguity in Panel B. As can be seen from Table 8, the values of the Trace IM test statistic for the linear specification substantially deviate from zero across all years, suggesting that the linear model is misspecified. The IOS_A test statistic reinforces the result, as their values in the case of the linear specification are found to be significantly more different from zero than those in the case of the log-linear specification. Based on these results, it can be concluded that the log-linear specification dominates the linear specification.

TABLE 8 Model specification test statistics

	Panel A: Queen contiguity				**Panel B: Rook contiguity**			
	Trace IM		IOS_A		Trace IM		IOS_A	
	Linear	Log-linear	Linear	Log-linear	Linear	Log-linear	Linear	Log-linear
2009	−23.280	0.191	29.800	5.831	−21.095	0.237	27.512	5.199
2010	−102.798	0.339	17.292	11.801	−99.757	0.281	16.512	9.465
2011	−95.008	0.114	19.117	12.197	−93.564	0.187	18.845	9.413
2012	−1560.199	0.278	48.810	14.573	−1552.325	0.134	48.360	12.207
2013	−618.555	0.160	18.447	14.981	−594.550	0.206	17.609	11.928
2014	−779.468	0.203	43.842	14.020	−753.519	0.136	41.853	11.064
2015	−569.047	0.430	31.230	13.109	−579.039	0.324	30.627	10.870
2016	−835.373	0.423	22.307	12.003	−755.002	0.376	21.717	10.028
2017	−809.996	0.442	17.641	13.003	−783.515	0.492	17.213	10.698
2018	−2628.956	0.509	35.722	14.809	−2338.951	0.416	33.083	12.225

Note: Trace IM test: $tr\big(\mathbf{J}(\theta_\mathbf{0}) - \mathbf{K}(\theta_\mathbf{0})\big) = 0$, IOS_A test: $tr\big(\mathbf{J}(\theta_\mathbf{0})^{-1}\mathbf{K}(\theta_\mathbf{0})\big) - p = 0$.

Comparing standard errors using those of the two information matrices (the diagonal elements of $\mathbf{J}(\theta_\mathbf{0})^{-1}$ and $\mathbf{K}(\theta_\mathbf{0})^{-1}$) is also able to provide evidence of model misspecification. In a correctly specified model, these standard errors should be in agreement. As the results reported in Table 9 indicate, it can be seen that this is obviously not the case for the linear specification, whereas there is better agreement with the log-linear

[13] More recently, Zhou et al. (2012) propose a test statistic that takes the form $tr(\mathbf{J}(\theta_\mathbf{0})^{-1}\mathbf{K}(\theta_\mathbf{0}))/p$, which is denoted as the information ratio (IR) test, and show that the statistic asymptotically follows a normal distribution.

specification.

TABLE 9 Standard errors for linear and log-linear models

		Panel A: Queen contiguity				**Panel B: Rook contiguity**			
		Linear		Log-linear		Linear		Log-linear	
		$\mathbf{J}(\theta_0)^{-1}$	$\mathbf{K}(\theta_0)^{-1}$	$\mathbf{J}(\theta_0)^{-1}$	$\mathbf{K}(\theta_0)^{-1}$	$\mathbf{J}(\theta_0)^{-1}$	$\mathbf{K}(\theta_0)^{-1}$	$\mathbf{J}(\theta_0)^{-1}$	$\mathbf{K}(\theta_0)^{-1}$
2009	α_0	0.037	0.063	0.124	0.109	0.036	0.065	0.119	0.108
	α_1	0.050	0.027	0.040	0.036	0.046	0.029	0.038	0.035
	σ	0.039	0.013	0.153	0.165	0.040	0.014	0.153	0.169
2010	α_0	0.022	0.041	0.190	0.164	0.021	0.040	0.174	0.152
	α_1	0.056	0.045	0.051	0.046	0.049	0.041	0.046	0.042
	σ	0.013	0.007	0.192	0.247	0.014	0.007	0.196	0.254
2011	α_0	0.024	0.047	0.181	0.158	0.023	0.046	0.164	0.148
	α_1	0.057	0.059	0.053	0.047	0.051	0.051	0.047	0.044
	σ	0.016	0.008	0.175	0.213	0.016	0.008	0.177	0.216
2012	α_0	0.015	0.026	0.190	0.175	0.015	0.025	0.176	0.168
	α_1	0.061	0.064	0.051	0.048	0.053	0.057	0.046	0.045
	σ	0.006	0.001	0.164	0.205	0.006	0.001	0.167	0.209
2013	α_0	0.015	0.025	0.201	0.190	0.015	0.024	0.184	0.173
	α_1	0.059	0.062	0.055	0.053	0.052	0.054	0.050	0.048
	σ	0.006	0.002	0.180	0.222	0.006	0.003	0.182	0.225
2014	α_0	0.017	0.029	0.201	0.188	0.017	0.028	0.183	0.175
	α_1	0.059	0.047	0.052	0.050	0.053	0.059	0.047	0.046
	σ	0.008	0.002	0.190	0.240	0.008	0.002	0.193	0.245
2015	α_0	0.016	0.023	0.199	0.167	0.015	0.023	0.183	0.159
	α_1	0.052	0.026	0.049	0.043	0.047	0.025	0.045	0.040
	σ	0.007	0.003	0.195	0.255	0.007	0.003	0.196	0.257
2016	α_0	0.013	0.021	0.177	0.153	0.013	0.020	0.167	0.150
	α_1	0.051	0.027	0.045	0.041	0.046	0.023	0.042	0.039
	σ	0.005	0.002	0.167	0.210	0.005	0.002	0.173	0.222
2017	α_0	0.013	0.023	0.186	0.160	0.012	0.022	0.173	0.151
	α_1	0.051	0.040	0.046	0.041	0.045	0.032	0.042	0.038
	σ	0.005	0.002	0.172	0.208	0.005	0.002	0.174	0.212
2018	α_0	0.012	0.021	0.198	0.165	0.012	0.021	0.184	0.160
	α_1	0.053	0.041	0.048	0.042	0.047	0.041	0.044	0.040
	σ	0.004	0.001	0.174	0.217	0.004	0.001	0.179	0.226

5.4 Pooling the Time-series and Cross-Section Data

Although the cross-sectional results show consistent evidence of the presence of spatially dependent volatility under multiple model specifications, the estimates point to the need to avoid unreliable conclusions by appropriately accounting for the time-varying heterogeneity that arises from unobserved factors to avoid unreliable conclusions. The rationale is provided in Figure 6, which plots the estimated time-varying spatial coefficients of α_1 together with the 95% pointwise confidence intervals obtained from the BC-SARCH and the final log-linear models over the 2009-2018 period, where the results reported in Panels (a) and (b) correspond to the queen and rook contiguity matrices, respectively. Figure 6 shows that, over the entire observed time period, the coefficient of α_1 was substantial and almost identical across the two models, irrespective of how the spatial weights are defined, indicating that neighborhood plays an important role in explaining volatility in the Chicago housing market. The magnitude of this effect, however, is not constant over time. The highest values of the coefficient were observed in 2009 after the outbreak of the financial crisis, after which values started to decrease in 2010 and reached their lowest level in 2013. After 2013, the coefficient exhibits a continuously increasing trend. In summary, the results indicate the varying but moderate persistence of the spatially-dependent volatility dynamics over the last decade in the Chicago housing market.

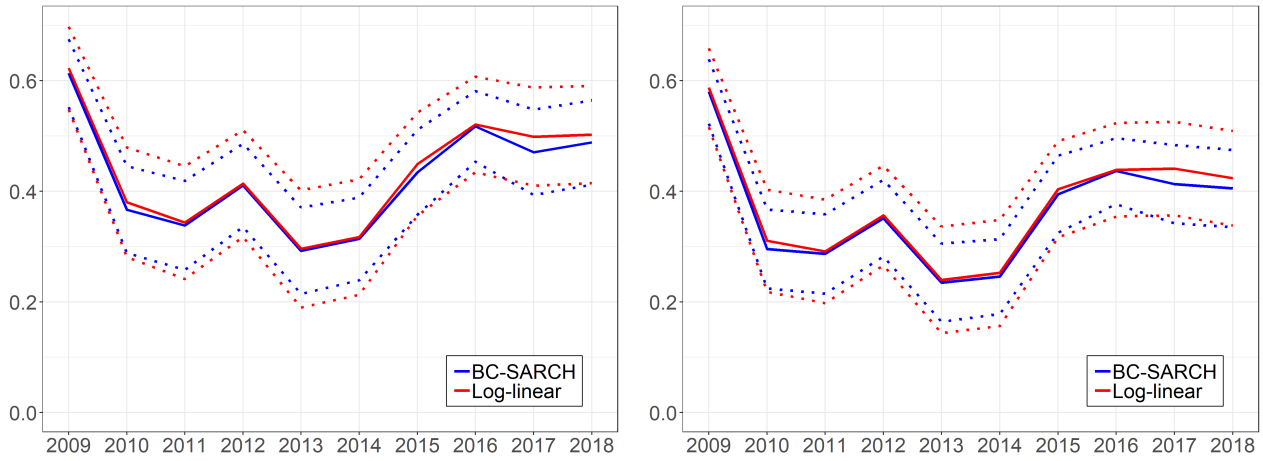

(a) Queen contiguity (b) Rook contiguity

FIGURE 6 Estimated spatial coefficients of α_1

In the finance literature, it has been well documented that the volatility of stock returns is higher during economic recessions (Schwert, 1989; Hamilton and Lin, 1996). As a result we observe high volatility clustering more frequently than low volatility, giving rise to an asymmetric pattern of volatility clustering. Recently, Ning et al. (2015) investigate the asymmetric pattern in volatility clustering for both the stock and foreign exchange

markets. They find evidence that the frequency probability of volatility clustering (for both high and low volatility) tends to increase during the crisis period. Figure 7 shows that the U.S. housing market has been no exception. The figure depicts the S&P Case-Shiller home price index (HPI) and the return data by taking the monthly change in the natural logarithm of the index for the U.S. in Panel (a) and for Chicago in Panel (b), respectively, with the shaded area representing the period of the financial crisis (2007-2009). As can be easily noticed, for both markets extreme return values are concentrated during the crisis, pointing to abnormally high volatility during this period. For both returns, the frequency of volatility clustering is also higher.

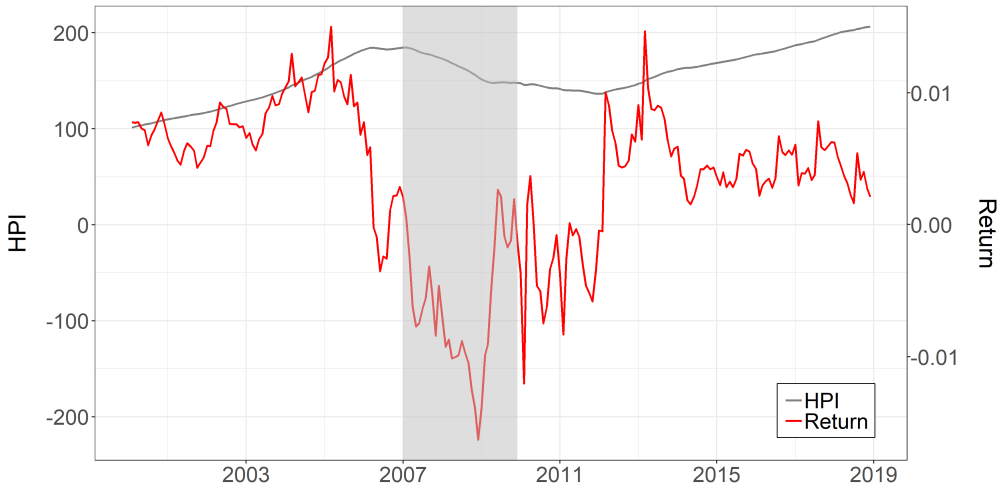

(a) U.S.

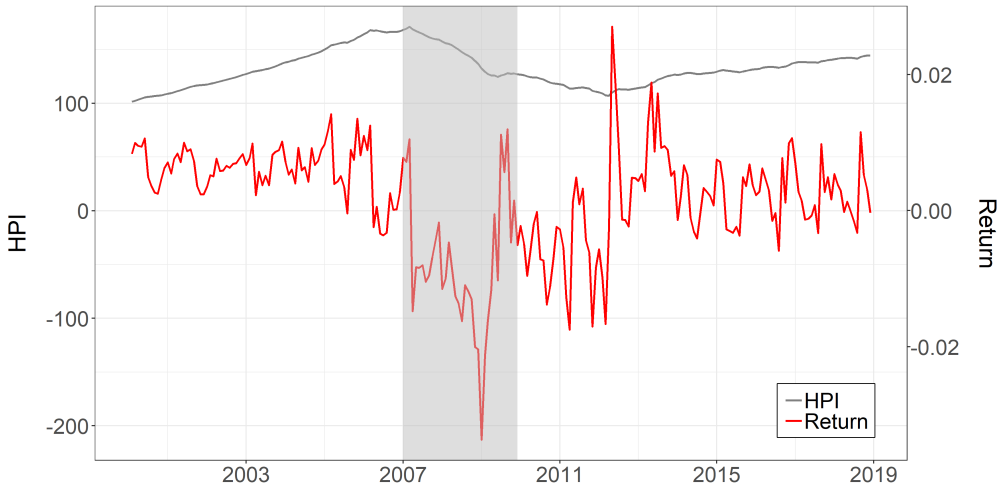

(b) Chicago

FIGURE 7 Home price index and its returns in the U.S. and Chicago

Several studies in the housing literature suggest that the degree to which volatility depends on spatial dependence also varies across market conditions. For example, Miao et al. (2011) show that spatial linkages

appear more intense during the active phase (1999–2006) than during the tranquil phase (1989–1998). Zhu et al. (2013) further define the period after 2006 as the crisis phase (2007-2009) and observe the increased intensity during the crisis period. Moreover, they find that, compared with spatial interactions that occur during tranquil and boom phases, spatial interdependence is much more distinct during the crisis. The present study suggests that such patterns identified at a large spatial scale (the MSA scale) remain similar at a much finer spatial scale (the census-tract scale). While the strongest spatial dependence of volatility between regions is detected during the financial crisis, a sizable increase in the dependence is also observed during the recent upturn that began in 2013 when housing prices started to recover from the declines recorded during the crisis. In this sense, the aspects of time-varying heterogeneity across census tracts have to be considered in the estimation, and adding the time-varying spatial effects to the regression model may be useful.

Many studies have examined temporal heterogeneity in standard panel data models, mostly on structural breaks or change points (e.g. Feng et al., 2008; Bai, 2010; Kim, 2011; Baltagi, Kao, et al., 2017). The spatial econometric literature has recently developed interest in heterogeneous spatial autoregressive panel data models, where the model parameters are heterogeneous, i.e. are different for distinct units in the sample (Aquaro et al., 2015; LeSage et al., 2017). The literature on temporal heterogeneity in spatial panel data models is, however, limited. Only a handful of studies have considered structural breaks in heterogeneous spatial panels. Sengupta (2017) considers hypothesis-testing for a structural change in a spatial panel model without fixed effects, while Li (2018) proposes and studies fixed-effects spatial panel data models with structural change using the quasi-maximum likelihood method. Some scholars in the finance literature have also attempted to make similar explorations of spatial panel data models with time-varying parameters. For example, Blasques et al. (2016) and Catania and Billé (2017) extend the spatial static panel data model by introducing time-varying spatial dependence, but their models are most suitable for a case with a large time dimension and a small cross-sectional dimension.

Very recently, Xu and Yang (2019) consider fixed-effects spatial panel data models with temporal heterogeneity in regressions and spatial coefficients by focusing on testing problems. They introduce a general method, the adjusted quasi score (AQS) method, for constructing the specification tests for temporal homogeneity/heterogeneity in regression and spatial coefficients in spatial panel data models, allowing for the existence of spatial and temporal heterogeneity in the intercepts (or fixed effects) of the model. This study presents the first application of their method to empirically test temporal heterogeneity in the spatial dependence of volatility, neighborhood elasticity in the log-linear model, in the housing market.

Changing notations to adapt to the changing context in which a dependent variable is log-squared returns and no explanatory variable is included as described in equation (4), first consider the following simplest panel

spatial lag model with individual specific fixed effects or one-way fixed effects (1FE-SL):

$$\log y_{it}^2 = \alpha_{0t} + \alpha_{1t} \sum_{j \neq i}^{n} w_{ij} \log y_{jt}^2 + u_i + z_{it}, \tag{19}$$

where α_{1t} is neighborhood elasticity at time t, u_i denotes the individual-specific fixed effects or the spatial heterogeneity in the intercept, and z_{it} is an $n \times 1$ vector of IID disturbances with mean zero and variance σ^2. As the aim of the present study is to test the hypothesis that neighborhood elasticity stays the same over time, only tests of temporal homogeneity in spatial coefficients, i.e. $H_0 : \alpha_{11} = \cdots = \alpha_{1T} = \alpha_1$, are conducted, allowing for the presence of unobserved cross-sectional heterogeneity in intercepts, i.e. the individual fixed effects u_i.

They further extend their tests to a panel spatial lag model with both individual and time-specific fixed effects or two-way fixed effects (2FE-SL), which can be written in the following form:

$$\log y_{it}^2 = \alpha_{0t} + \alpha_{1t} \sum_{j \neq i}^{n} w_{ij} \log y_{jt}^2 + u_i + v_t + z_{it}, \tag{20}$$

where v_t are the unobserved time-specific effects or the unobserved temporal heterogeneity in the intercept. Based on these models, two types of AQS tests (naive and robust) are proposed and these tests are fully extended to the spatial panel data models with both spatial lag and error (SLE) dependence, where the disturbances are also subject to spatial interactions. However, since they show that the robust tests have much superior finite and large sample properties than the native tests through Monte Carlo simulation, and a model specification search is not of primary interest in the present study, only asymptotically valid and non-normality robust AQS tests and spatial lag models given in equations (19) and (20) are considered.

As the proposed tests are intended for balanced panel data, only census tracts that have the same number of time observations are included to obtain a balanced panel. The purpose of constructing the pseudo-panel data is to model time heterogeneity and make full use of information in the data, improving the accuracy and efficiency of estimation.[14] The resulting pseudo-panel consists of a total of 716 census tracts over 10 time periods between 2009 and 2018. The special weight matrices are based on queen and rook contiguity matrices, and then row-normalized as before.

Coming back to Figure 6, it can be suggested that around the year 2013, there is a shift in the estimated value of neighborhood elasticity α_1. Thus, the tests are conducted on the full period (2009-2018) and two sub-periods (2009-2013 and 2014-2018). The 2009-2013 period is further broken down into two sub-periods,

[14] Most existing spatial panel estimation methods are designed for balanced panel data, and are not effective for unbalanced panels because of the computational burden associated with inverting a large spatial weighting matrix.

2009-2010 and 2011-2013, to examine whether the structure changes during the initial recovery phase after the financial crisis. Table 10 summarizes the values of the test statistics and their p-values for the robust AQS tests for temporal homogeneity based on both the full period and several sub-periods, fitted using the two models: a one-way fixed-effects spatial lag model (1FE-SL) and a two-way fixed-effects spatial lag model (2FE-SL).

TABLE 10 Tests for temporal homogeneity of neighborhood elasticity

	Panel A: Queen contiguity		**Panel B: Rook contiguity**	
	1FE-SL	2FE-SL	1FE-SL	2FE-SL
$t_1 - t_{10}$ (2009-2018)	152.302	12.030	160.863	8.949
	(0.000)	(0.212)	(0.000)	(0.442)
$t_1 - t_5$ (2009-2013)	60.308	8.891	64.414	3.258
	(0.000)	(0.064)	(0.000)	(0.516)
$t_6 - t_{10}$ (2014-2018)	16.184	5.528	16.890	6.224
	(0.003)	(0.237)	(0.002)	(0.183)
$t_1 - t_2$ (2009-2010)	34.923	0.115	39.256	0.160
	(0.000)	(0.735)	(0.000)	(0.690)
$t_3 - t_5$ (2011-2013)	14.679	5.938	13.163	3.665
	(0.001)	(0.051)	(0.001)	(0.160)

Note: p-values appear in parentheses in every second row. 1FE-SL: one-way fixed-effects spatial lag model; 2FE-SL: two-way fixed-effects spatial lag model.

From the abovementioned results it can be seen that, when the 1FE-SL is applied, i.e. temporal heterogeneity in intercepts is not controlled for, tests based on the full data clearly reject the null hypothesis of temporal homogeneity in neighborhood elasticity. To test whether the null hypothesis holds when 2013 is a change point, the same set of tests is applied to the two sub-periods, 2009-2013 and 2014-2018. The resulting statistics reject the null hypothesis and exhibit no change point. The results for 2009-2010 and 2011-2013 are also fairly stable, consistently rejecting the null hypothesis. Overall, a rejection of the null hypothesis in any sub-period indicates that neighborhood elasticity is temporally heterogeneous and it seems to stem from full heterogeneity instead of the existence of change points.

When the 2FE-SL model is applied, however, the null hypothesis of homogeneity of neighborhood elasticity is not rejected in either full period or any sub-period. This suggests that, when the time fixed effect is taken into account, neighborhood elasticity becomes homogeneous. It is important to note that when the null hypothesis of homogeneity is accepted in the full period, tests for sub-periods are redundant in the sense that acceptance of the null hypothesis for full period also results in accepting the null hypothesis for any sub-period. Nonetheless, the test results for the sub-periods lend further support to the homogeneity of neighborhood elasticity. These findings

hold irrespective of the spatial weight matrix used. In summary, the test results show that, after controlling for both spatial and temporal heterogeneity in the intercepts, the homogeneity of neighborhood elasticity is achieved and there exists no structural change in the term, and moreover a homogeneous spatial panel data model can be used and specifying change points is not necessary.

6 Robustness and Sensitivity Analysis

6.1 Alternative Volatility Measure

Although the estimation of the spatial dependence parameter for the BC-SARCH model is based on the squared returns, many researchers have relied on other measures of volatility such as absolute returns.[15] To ensure that the results are not sensitive to the underlying measurement concepts, it is necessary to repeat the procedure with the alternative measures of volatility. Therefore, the estimation of the BC-SARCH model is repeated with absolute returns. Interestingly, the absolute returns tend to result in equally strong evidence for spatially dependent volatility. This is to be expected, as squared returns are a simple one-to-one transformation of absolute returns, so if squared returns have spatially dependent volatility features, then so will absolute returns. Indeed, Figure 8 shows almost identical spatial patterns for both squared returns and absolute returns.

To confirm this expectation, the following modification of the BC-SARCH model is specified:

$$\frac{|y_i|^\lambda - 1}{\lambda} = \alpha_0 + \alpha_1 \sum_{j \neq i}^{n} w_{ij} \frac{|y_j|^\lambda - 1}{\lambda} + \epsilon_i, \tag{21}$$

where $|y_i|$ denotes the absolute returns at location i and $|y_j|$ denotes the values at surrounding locations j ($j \neq i$).

Table 11 presents the results obtained when the model is estimated with the same econometric methodology as in Section 3, but the absolute returns are used as the dependent variable. The results coincide with those derived earlier in Table 5 using the squared returns. The coefficient on α_1 remains almost unchanged in both magnitude and statistical significance when using absolute returns by suitably rescaling the transformation parameter λ. Adjusted in accordance with the transformation, the estimates of λ are now almost twice as large when using absolute returns than using squared returns, and thus the test statistic for the null hypothesis that $\lambda = 0$ becomes highly significant. These findings also hold irrespective of the choice of the spatial weight matrix. Altogether, the results suggest that the alternative measure of volatility exhibits a similar ability to detect the spatial volatility clustering behavior.

[15] Squared returns have been employed by Lobato and Savin (1998), Gil-Alana (2003), Cavalcante and Assaf (2004), Cotter (2005) and Elder and Jin (2007), whereas absolute returns have been used by Ding and Granger (1996), Sibbertsen (2004) and others.

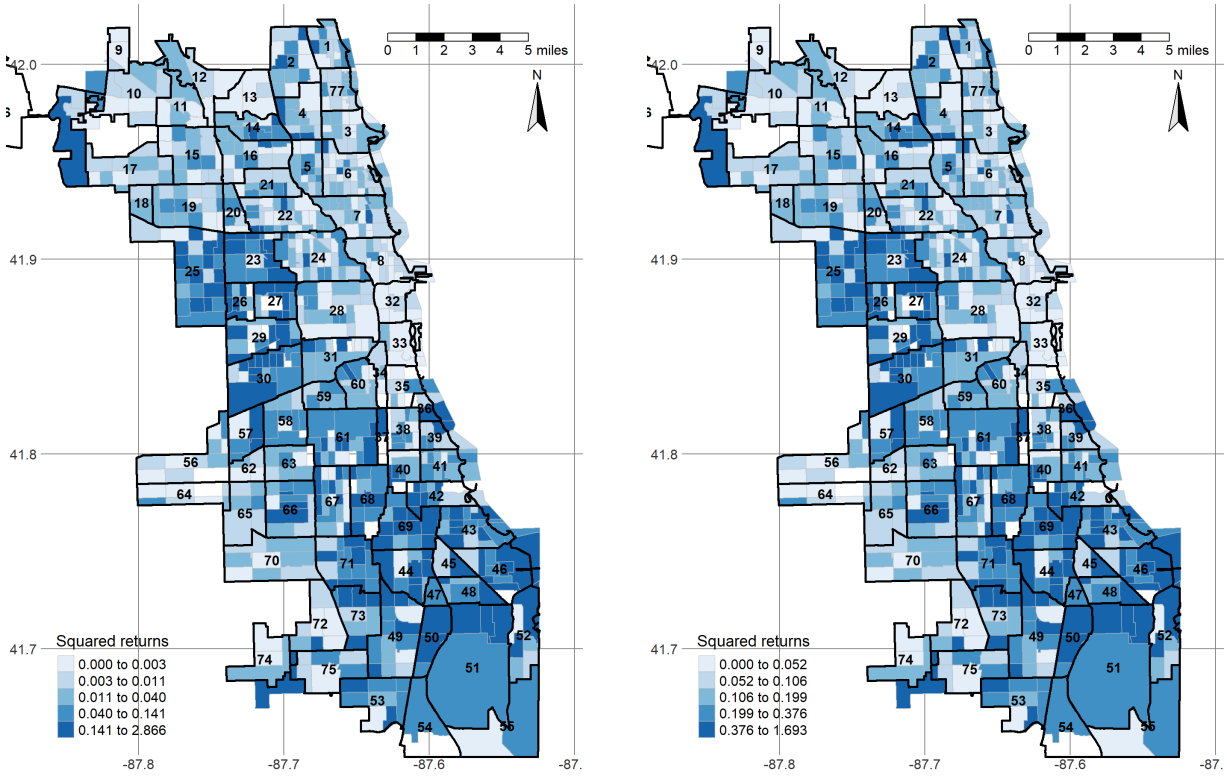

(a) Squared Returns (b) Absolute Returns

FIGURE 8 Spatial distribution of (a) squared returns and (b) absolute returns, 2017

Note: The listed numbers refer to the codes for Chicago community areas (see Table 13 in the Appendix for details).

6.2 Alternative Spatial Weight Matrix

To further confirm that the estimates are robust to alternative weight matrices, three distance-based spatial weight matrices are used in addition to the simple contiguity matrices: (a) fixed distance band, (b) inverse distance, and (c) inverse distance squared. With the fixed distance band method, $w_{ij} = 1$ if $d_{ij} \leq C$ and zero if $d_{ij} > C$, while in the inverse distance method, $w_{ij} = 1/d_{ij}^k$ if $d_{ij} \leq C$ and zero if $d_{ij} > C$, where C is a distance cutoff beyond which no spatial relationship is assumed, d_{ij} is the distance in miles between the centroids of census tracts i and j, and k is a dampening coefficient whose magnitude determines how quickly the spatial relationship between a tract and its neighbors declines with distance. The inverse distance method allows neighbors located closer to each other to have higher weights than neighbors located far away from each other. These weight matrices are also row-normalized. Here, the value of C is set equal to 3 (miles) between census-tract centroids such that every census tract has at least one neighbor, and k is set equal to 1 and 2 to implement inverse distance and inverse distance squared matrices, respectively. These weight matrices are also row-normalized.

Space limitations prevent me from comparing the entire estimation output for the three alternative cases, so the focus here is exclusively on the specific estimates for the key parameters, α_1 and λ for the BC-SARCH

TABLE 11 BC-SARCH model ML estimation results using absolute returns

	2009	2010	2011	2012	2013	2014	2015	2016	2017	2018
Panel A: Queen contiguity										
α_0	−0.402***	−0.869***	−0.861***	−0.802***	−0.887***	−0.934***	−0.827***	−0.646***	−0.758***	−0.774***
	(0.050)	(0.071)	(0.073)	(0.067)	(0.065)	(0.068)	(0.071)	(0.061)	(0.069)	(0.076)
α_1	0.614***	0.373***	0.330***	0.410***	0.291***	0.317***	0.439***	0.512***	0.467***	0.490***
	(0.028)	(0.031)	(0.038)	(0.032)	(0.031)	(0.031)	(0.029)	(0.027)	(0.029)	(0.032)
σ	0.463***	0.593***	0.527***	0.421***	0.409***	0.476***	0.552***	0.383***	0.421***	0.450***
	(0.005)	(0.005)	(0.007)	(0.006)	(0.004)	(0.005)	(0.005)	(0.004)	(0.006)	(0.008)
λ	0.279***	0.265***	0.260***	0.264***	0.323***	0.285***	0.264***	0.305***	0.284***	0.250***
	(0.033)	(0.046)	(0.042)	(0.032)	(0.031)	(0.037)	(0.045)	(0.031)	(0.037)	(0.044)
n	759	766	766	761	763	769	776	766	765	767
Log-likelihood	-4.7	238.7	148.8	295.2	240.6	289.7	356.8	328.2	374.7	418.8
Pseudo R^2	0.311	0.115	0.075	0.109	0.071	0.070	0.159	0.214	0.217	0.198
Moran's I	−0.045	−0.017	−0.012	−0.018	−0.009	−0.018	−0.025	−0.034	−0.034	−0.021
(p-value)	(0.982)	(0.774)	(0.691)	(0.787)	(0.651)	(0.787)	(0.873)	(0.944)	(0.945)	(0.830)
J-B	18.293	1.377	5.442	1.685	2.351	1.450	0.527	2.580	3.778	1.737
(p-value)	(0.000)	(0.502)	(0.066)	(0.431)	(0.309)	(0.484)	(0.768)	(0.275)	(0.151)	(0.420)
Panel B: Rook contiguity										
α_0	−0.446***	−1.050***	−0.904***	−0.946***	−1.011***	−1.071***	−0.959***	−0.768***	−0.880***	−0.932***
	(0.054)	(0.087)	(0.074)	(0.083)	(0.087)	(0.083)	(0.091)	(0.067)	(0.093)	(0.088)
α_1	0.583***	0.290***	0.325***	0.351***	0.243***	0.257***	0.395***	0.456***	0.418***	0.410***
	(0.030)	(0.036)	(0.036)	(0.036)	(0.037)	(0.034)	(0.035)	(0.028)	(0.033)	(0.033)
σ	0.491***	0.725***	0.582***	0.521***	0.496***	0.558***	0.672***	0.461***	0.499***	0.524***
	(0.016)	(0.017)	(0.017)	(0.023)	(0.023)	(0.018)	(0.020)	(0.015)	(0.022)	(0.019)
λ	0.235***	0.189**	0.214***	0.192**	0.235***	0.223***	0.191*	0.239***	0.228**	0.214**
	(0.050)	(0.091)	(0.068)	(0.077)	(0.078)	(0.078)	(0.104)	(0.060)	(0.093)	(0.084)
n	759	766	766	761	763	769	776	766	765	767
Log-likelihood	-6.3	232.4	145.8	289.9	237.5	284.5	355.6	316.1	370.1	407.5
Pseudo R^2	0.317	0.095	0.062	0.097	0.057	0.054	0.154	0.180	0.206	0.158
Moran's I	−0.044	−0.021	−0.016	−0.019	−0.008	−0.019	−0.024	−0.044	−0.039	−0.033
(p-value)	(0.956)	(0.789)	(0.722)	(0.761)	(0.612)	(0.766)	(0.832)	(0.960)	(0.941)	(0.903)
J-B	11.433	1.205	5.249	1.593	1.763	1.646	0.273	1.074	3.001	0.661
(p-value)	(0.003)	(0.548)	(0.072)	(0.451)	(0.414)	(0.439)	(0.873)	(0.585)	(0.223)	(0.719)

Note: For $H_0 : \lambda = 1$, the null is rejected in all cases. Standard errors appear in parentheses. Pseudo R^2 is computed as the squared correlation between the observed and predicted values of the dependent variable (Anselin, 1988). Diagnostic tests including Moran's I test and the J-B (Jarque–Bera) test are implemented to examine the spatial dependence and normality of the residuals. *** $p < 0.01$; ** $p < 0.05$; * $p < 0.1$

model and α_1 for the log-linear model. In Table 12 I report the estimation results for both the BC-SARCH and log-linear models. The results reported in columns 1 and 2 confirm the validity of the BC-SARCH model in describing the spatial dependence pattern in volatility. The signs and significance of the spatial dependence parameter α_1 are consistent with those reported in Table 5, although the magnitude appears to be larger compared with simple contiguity. This is expected, as the distance between the centroids of census tracts is determined to ensure that larger census tracts are connected and have at least one neighbor, leading smaller census tracts

to have many other smaller census tracts as neighbors. The results also provide further support for the log-linear model that is determined by the transformation parameter λ. The parameter estimates remain substantially the same across specifications, with values around zero over the entire study period. Finally, the log-linear model estimation results are given in column 3 and reveal that the coefficients of α_1 retain the same signs and significance levels as the BC-SARCH model, with only minor differences in magnitude. In sum, the results of the estimations presented in Table 12 are essentially consistent with the results presented in Table 5 and Table 6, proving the robustness and objectivity of the results.

7 Conclusion

Reducing housing price volatility has emerged as a critical challenge for housing policy-makers as higher housing price volatility levels may discourage newly formed households from committing to homeownership. To develop effective policies to better protect households from the consequences of volatility, an important task for policy-makers and academics is to understand the nature and extent of housing price volatility. This paper studies spatial variation of volatility in the Chicago housing market by proposing a flexible spatial volatility model for squared returns based on a Box-Cox transformation, a technique that has been frequently used as both a flexible functional form and as a decision device to distinguish between alternative model specifications. To estimate the proposed model, an MLE procedure is employed to simultaneously estimate the transformation parameter and the analytical form of spatial dependence in volatility.

The estimation results suggest that housing returns in Chicago show strong spatial dependence in volatility and the commonly used log-linear functional form is appropriate, irrespective of variations in neighborhood criteria. The appropriateness of the log-linear model is also determined through associated model diagnostics and specification tests. This result has important economic implications for both researchers and housing market practitioners. In the final log-linear model, a new practical indicator is proposed. Neighborhood elasticity, captured by the parameter α_1 in the model, provides a measure of how volatility in one neighborhood is linked to that in surrounding neighborhoods. The average annual elasticity is found to be 0.4 across spatial weight matrices, which can be used as a benchmark for comparing housing markets. The findings have important practical implications. The spatial volatility clustering can be used in the forecasting context to obtain appropriate confidence interval and thus helps policy-makers develop strategies to mitigate the impacts of volatility transmission and the risk of contagion in the housing market. Finally, to identify whether neighborhood elasticity remains constant over time, adjusted quasi score (AQS) tests for testing the presence of temporal heterogeneity in spatial parameters in spatial panel data models are considered. The test results reveal that

TABLE 12 Estimation results using alternative spatial weight matrix specifications

	BC-SARCH				Log-linear	
	α_1		λ		α_1	
Panel A: Fixed distance band						
2009	0.927***	(0.048)	0.107	(0.227)	0.933***	(0.034)
2010	0.830***	(0.075)	0.094	(0.406)	0.847***	(0.064)
2011	0.768***	(0.086)	0.109	(0.307)	0.785***	(0.081)
2012	0.860***	(0.065)	0.104	(0.305)	0.867***	(0.058)
2013	0.788***	(0.085)	0.133	(0.298)	0.792***	(0.079)
2014	0.859***	(0.070)	0.115	(0.360)	0.862***	(0.059)
2015	0.902***	(0.064)	0.093	(0.492)	0.908***	(0.043)
2016	0.921***	(0.048)	0.124	(0.287)	0.923***	(0.038)
2017	0.910***	(0.053)	0.111	(0.378)	0.921***	(0.039)
2018	0.916***	(0.056)	0.101	(0.451)	0.922***	(0.038)
Panel B: Inverse distance						
2009	0.930***	(0.043)	0.115	(0.205)	0.935***	(0.030)
2010	0.796***	(0.067)	0.096	(0.398)	0.814***	(0.063)
2011	0.748***	(0.075)	0.110	(0.298)	0.760***	(0.074)
2012	0.812***	(0.059)	0.104	(0.300)	0.817***	(0.062)
2013	0.734***	(0.072)	0.135	(0.294)	0.736***	(0.079)
2014	0.791***	(0.062)	0.117	(0.358)	0.796***	(0.067)
2015	0.854***	(0.057)	0.096	(0.489)	0.863***	(0.051)
2016	0.889***	(0.044)	0.125	(0.279)	0.891***	(0.044)
2017	0.877***	(0.049)	0.116	(0.384)	0.890***	(0.044)
2018	0.877***	(0.050)	0.104	(0.443)	0.884***	(0.046)
Panel C: Inverse distance squared						
2009	0.841***	(0.036)	0.124	(0.190)	0.847***	(0.039)
2010	0.584***	(0.054)	0.098	(0.412)	0.612***	(0.066)
2011	0.549***	(0.057)	0.109	(0.302)	0.558***	(0.071)
2012	0.617***	(0.050)	0.103	(0.308)	0.625***	(0.065)
2013	0.500***	(0.054)	0.136	(0.305)	0.503***	(0.075)
2014	0.538***	(0.050)	0.116	(0.385)	0.548***	(0.072)
2015	0.664***	(0.048)	0.098	(0.517)	0.681***	(0.059)
2016	0.735***	(0.038)	0.125	(0.287)	0.735***	(0.053)
2017	0.716***	(0.044)	0.118	(0.419)	0.735***	(0.053)
2018	0.719***	(0.043)	0.103	(0.448)	0.730***	(0.054)

Note: Standard errors appear in parentheses. $^{***}\ p < 0.01$; $^{**}\ p < 0.05$; $^{*}\ p < 0.1$

neighborhood elasticity becomes homogeneous after controlling for both spatial and temporal heterogeneity in the intercepts of the model.

References

Anari, A. and J. Kolari (2002). House prices and inflation. *Real Estate Economics* 30, 67–84.

Andersen, T. G., T. Bollerslev, F. X. Diebold, and H. Ebens (2001). The distribution of realized stock return volatility. *Journal of financial economics* 61, 43–76.

Anselin, L. (1988). *Spatial econometrics: methods and models*. Springer Science & Business Media.

Aquaro, M., N. Bailey, and M. H. Pesaran (2015). Quasi maximum likelihood estimation of spatial models with heterogeneous coefficients. *USC-INET Research Paper* 15-17.

Arrow, K. J., H. B. Chenery, B. S. Minhas, and R. M. Solow (1961). Capital-labor substitution and economic efficiency. *Review of Economics and Statistics*, 225–250.

Bai, J. (2010). Common breaks in means and variances for panel data. *Journal of Econometrics* 157, 78–92.

Bailey, M. J., R. F. Muth, and H. O. Nourse (1963). A regression method for real estate price index construction. *Journal of the American Statistical Association* 58, 933–942.

Baltagi, B. H., C. Kao, and L. Liu (2017). Estimation and identification of change points in panel models with nonstationary or stationary regressors and error term. *Econometric Reviews* 36, 85–102.

Baltagi, B. H. and D. Li (2004). Testing for linear and log-linear models against Box-Cox alternatives with spatial lag dependence, 35–74.

Barndorff-Nielsen, O. E. and N. Shephard (2005). How accurate is the asymptotic approximation to the distribution of realized variance. *Identification and inference for econometric models. A Festschrift in honour of TJ Rothenberg*, 306–311.

Barros, C. P., L. A. Gil-Alana, and J. E. Payne (2015). Modeling the long memory behavior in US housing price volatility. *Journal of Housing Research* 24, 87–106.

Bera, A. K. and P. Simlai (2005). Testing spatial autoregressive model and a formulation of spatial ARCH (SARCH) model with applications. *Econometric Society World Congress, London*.

Blasques, F., S. J. Koopman, A. Lucas, and J. Schaumburg (2016). Spillover dynamics for systemic risk measurement using spatial financial time series models. *Journal of Econometrics* 195, 211–223.

Bogin, A., W. Doerner, and W. Larson (2019). Local house price dynamics: New indices and stylized facts. *Real Estate Economics* 47, 365–398.

Bollerslev, T., R. Y. Chou, and K. F. Kroner (1992). ARCH modeling in finance: A review of the theory and empirical evidence. *Journal of econometrics* 52, 5–59.

Borovkova, S. and R. Lopuhaa (2012). Spatial GARCH: A spatial approach to multivariate volatility modeling. *Working paper*.

Box, G. E. and D. R. Cox (1964). An analysis of transformations. *Journal of the Royal Statistical Society: Series B (Methodological)* 26, 211–243.

Breitung, J. and C. Wigger (2018). Alternative GMM estimators for spatial regression models. *Spatial Economic Analysis*, 148–170.

Cannon, S., N. G. Miller, and G. S. Pandher (2006). Risk and Return in the US Housing Market: A Cross-Sectional Asset-Pricing Approach. *Real Estate Economics* 34, 519–552.

Caporin, M. and P. Paruolo (2006). GARCH models with spatial structure. *SIS Statistica*, 447–450.

Capozza, D. R., P. H. Hendershott, and C. Mack (2004). An anatomy of price dynamics in illiquid markets: analysis and evidence from local housing markets. *Real Estate Economics* 32, 1–32.

Case, K. E. and R. J. Shiller (1987). Prices of single family homes since 1970: New indexes for four cities.

Case, K. E. and R. J. Shiller (1988). The efficiency of the market for single-family homes.

Catania, L. and A. G. Billé (2017). Dynamic spatial autoregressive models with autoregressive and heteroskedastic disturbances. *Journal of Applied Econometrics* 32, 1178–1196.

Cavalcante, J. and A. Assaf (2004). Long range dependence in the returns and volatility of the Brazilian stock market. *European Review of Economics and Finance* 3, 22.

Cilluffo, A., A. Geiger, and R. Fry (2017). More US households are renting than at any point in 50 years. *Pew Research Center*. https://www.pewresearch.org/fact-tank/2017/07/19/more-u-s-households-are-renting-than-at-any-point-in-50-years/.

Clapp, J. M., C. Giaccotto, and D. Tirtiroglu (1991). Housing price indices based on all transactions compared to repeat subsamples. *Real Estate Economics* 19, 270–285.

Corsi, F. (2009). A simple approximate long-memory model of realized volatility. *Journal of Financial Econometrics* 7, 174–196.

Cotter, J. (2005). Uncovering long memory in high frequency UK futures. *European Journal of Finance* 11, 325–337.

Crawford, G. W. and M. C. Fratantoni (2003). Assessing the forecasting performance of regime-switching, ARIMA and GARCH models of house prices. *Real Estate Economics* 31, 223–243.

Ding, Z. and C. W. Granger (1996). Modeling volatility persistence of speculative returns: a new approach. *Journal of econometrics* 73, 185–215.

Dolde, W. and D. Tirtiroglu (1997). Temporal and spatial information diffusion in real estate price changes and variances. *Real Estate Economics* 25, 539–565.

Elder, J. and H. J. Jin (2007). Long memory in commodity futures volatility: A wavelet perspective. *Journal of Futures Markets: Futures, Options, and Other Derivative Products* 27, 411–437.

Feng, Q., C. Kao, and S. Lazarová (2008). Estimation and identification of change points in panel models. *Center for Policy Research, Syracuse University, Mimeo*.

Fuller, W. A. (1996). *Introduction to statistical time series*. John Wiley & Sons.

Gil-Alana, L. (2003). Fractional integration in the volatility of asset returns.

Gonçalves, S. and N. Meddahi (2011). Box–Cox transforms for realized volatility. *Journal of Econometrics* 160, 129–144.

Hamilton, J. D. and G. Lin (1996). Stock market volatility and the business cycle. *Journal of applied econometrics* 11, 573–593.

Hansen, P. R., Z. Huang, and H. H. Shek (2012). Realized garch: a joint model for returns and realized measures of volatility. *Journal of Applied Econometrics* 27, 877–906.

Hayunga, D. K., R. K. Pace, and S. Zhu (2019). Borrower risk and housing price appreciation. *Journal of Real Estate Finance Economics*, 1–23.

Hossain, B. and E. Latif (2009). Determinants of housing price volatility in Canada: a dynamic analysis. *Applied Economics* 41.27, 3521–3531.

Islam, S. M., S. Watanapalachaikul, and C. Clark (2007). Some tests of the efficiency of the emerging financial markets: An analysis of the Thai stock market. *Journal of Emerging Market Finance* 6, 291–302.

Karoglou, M., B. Morley, and D. Thomas (2013). Risk and structural instability in US house prices. *The Journal of Real Estate Finance and Economics* 46.3, 424–436.

Kelejian, H. H. and I. R. Prucha (1999). A generalized moments estimator for the autoregressive parameter in a spatial model. *International economic review* 40, 509–533.

Kelejian, H. H. and I. R. Prucha (2010). Specification and estimation of spatial autoregressive models with autoregressive and heteroskedastic disturbances. *Journal of econometrics* 157, 53–67.

Kim, D. (2011). Estimating a common deterministic time trend break in large panels with cross sectional dependence. *Journal of Econometrics* 164, 310–330.

Koopman, S. J. and M. Scharth (2012). The analysis of stochastic volatility in the presence of daily realized measures. *Journal of Financial Econometrics* 11, 76–115.

Lee, C. L. (2009). Housing price volatility and its determinants. *International Journal of Housing Markets and Analysis*.

Lee, C. L. and R. Reed (2013). Volatility decomposition of Australian housing prices. *Journal of Housing Research* 23.1, 21–43.

Lee, L.-F. (2004). Asymptotic distributions of quasi-maximum likelihood estimators for spatial autoregressive models. *Econometrica* 72.6, 1899–1925.

LeSage, J. P., C. Vance, and Y.-Y. Chih (2017). A Bayesian heterogeneous coefficients spatial autoregressive panel data model of retail fuel duopoly pricing. *Regional Science and Urban Economics* 62, 46–55.

Li, D. and C. Le (2010). Nonlinearity and spatial lag dependence: tests based on double-length regressions. *Journal of Time Series Econometrics* 2.

Li, K. (2018). Spatial panel data models with structural change.

Lin, P.-t. and F. Fuerst (2014). Volatility clustering, risk-return relationship, and asymmetric adjustment in the Canadian housing market. *Journal of Real Estate Portfolio Management* 20.1, 37–46.

Lobato, I. N. and N. E. Savin (1998). Real and spurious long-memory properties of stock-market data. *Journal of Business & Economic Statistics* 16, 261–268.

McMillen, D. P. (2012). Repeat sales as a matching estimator. *Real Estate Economics* 40, 745–773.

Miao, H., S. Ramchander, and M. W. Simpson (2011). Return and volatility transmission in US housing markets. *Real Estate Economics* 39, 701–741.

Miles, W. (2008). Volatility clustering in US home prices. *Journal of Real Estate Research* 30, 73–90.

Miles, W. (2011). Long-range dependence in US home price volatility. *Journal of Real Estate Finance and Economics* 42, 329–347.

Miller, N. and L. Peng (2006). Exploring metropolitan housing price volatility. *Journal of Real Estate Finance and Economics* 33, 5–18.

Ning, C., D. Xu, and T. S. Wirjanto (2015). Is volatility clustering of asset returns asymmetric? *Journal of Banking & Finance* 52, 62–76.

Nugroho, D. B. and T. Morimoto (2016). Box–Cox realized asymmetric stochastic volatility models with generalized Student's t-error distributions. *Journal of Applied Statistics* 43, 1906–1927.

Otto, P., W. Schmid, and R. Garthoff (2018). Generalised spatial and spatiotemporal autoregressive conditional heteroscedasticity. *Spatial Statistics* 26, 125–145.

Oxley, M. and M. Haffner (2010). Housing taxation and subsidies: international comparisons and the options for reform. *JRF programme paper: Housing Market Taskforce*.

Piras, G. and I. R. Prucha (2014). On the finite sample properties of pre-test estimators of spatial models. *Regional Science and Urban Economics* 46, 103–115.

Presnell, B. and D. D. Boos (2004). The IOS test for model misspecification. *Journal of the American Statistical Association* 99, 216–227.

Sarwar, G. and W. Khan (2017). The effect of US stock market uncertainty on emerging market returns. *Emerging Markets Finance and Trade* 53, 1796–1811.

Sato, T. and Y. Matsuda (2020). Spatial extension of generalized autoregressive conditional heteroskedasticity models. *Spatial Economic Analysis*, 1–13.

Schwert, G. W. (1989). Why does stock market volatility change over time? *Journal of Finance* 44, 1115–1153.

Sengupta, A. (2017). Testing for a structural break in a spatial panel model. *Econometrics* 5, 12.

Sibbertsen, P. (2004). Long memory in volatilities of German stock returns. *Empirical Economics* 29, 477–488.

Solow, R. M. (1956). A contribution to the theory of economic growth. *Quarterly journal of economics* 70, 65–94.

Stephens, M. (2011). *Tackling housing market volatility in the UK*. Joseph Rowntree Foundation York.

Stevenson, S. (1999). The performance and inflation hedging ability of regional housing markets. *Journal of Property Investment & Finance* 17, 239–260.

Stevenson, S., P. J. Wilson, and R. Zurbruegg (2007). Assessing the time-varying interest rate sensitivity of real estate securities. *The European Journal of Finance*, 705–715.

Taşpınar, S., O. Doğan, and A. K. Bera (2019). Heteroskedasticity-consistent covariance matrix estimators for spatial autoregressive models. *Spatial Economic Analysis*, 241–268.

Taylor, N. (2017). Realised variance forecasting under Box-Cox transformations. *International Journal of Forecasting* 33, 770–785.

Weigand, R. (2014). Matrix Box-Cox models for multivariate realized volatility.

White, H. (1982). Maximum likelihood estimation of misspecified models. *Econometrica: Journal of the Econometric Society*, 1–25.

Willcocks, G. (2010). Conditional variances in UK regional house prices. *Spatial Economic Analysis*, 339–354.

Xu, Y. and Z. Yang (2019). Specification tests for temporal heterogeneity in spatial panel models with fixed effects.

Zheng, T. and T. Song (2014). A realized stochastic volatility model with Box–Cox transformation. *Journal of Business & Economic Statistics* 32, 593–605.

Zhou, Q. M., P. X.-K. Song, and M. E. Thompson (2012). Information ratio test for model misspecification in quasi-likelihood inference. *Journal of the American Statistical Association* 107, 205–213.

Zhu, B., R. Füss, and N. B. Rottke (2013). Spatial linkages in returns and volatilities among US regional housing markets. *Real Estate Economics* 41, 29–64.

A Appendix

A.1 Analytical Derivatives for the BC-SARCH Process

The terms of the Hessian are the second and cross derivatives of equation (10) with respect to the parameter vector θ, resulting in

$$\frac{\partial^2 \log L}{\partial \alpha_0^2} = -\frac{n}{\sigma^2} \tag{22}$$

$$\frac{\partial^2 \log L}{\partial \alpha_0 \partial \alpha_1} = -\frac{1}{\sigma^2} l' W y^{2(\lambda)} \tag{23}$$

$$\frac{\partial^2 \log L}{\partial \alpha_0 \partial \lambda} = \frac{1}{\sigma^2} \mathbf{1}' \left[(I - \alpha_1 W) \frac{\partial y^{2(\lambda)}}{\partial \lambda} \right] \tag{24}$$

$$\frac{\partial^2 \log L}{\partial \alpha_0 \partial \sigma^2} = -\frac{1}{\sigma^4} \mathbf{1}' \epsilon \stackrel{E}{=} 0 \tag{25}$$

$$\frac{\partial^2 \log L}{\partial \alpha_1^2} = \frac{1}{\sigma^2} (W y^{2(\lambda)})' W y^{2(\lambda)} - \sum_{i=1}^{n} \frac{\omega_i^2}{(1 - \alpha_1 \omega_i)^2} \tag{26}$$

$$\frac{\partial^2 \log L}{\partial \alpha_1 \partial \lambda} = \frac{1}{\sigma^2} \left(W \frac{\partial y^{2(\lambda)}}{\partial \lambda} \right)' \epsilon + \frac{1}{\sigma^2} (W y^{2(\lambda)})' \left[(I - \alpha_1 W) \frac{\partial y^{2(\lambda)}}{\partial \lambda} \right] \tag{27}$$

$$\frac{\partial^2 \log L}{\partial \alpha_1 \partial \sigma^2} = -\frac{1}{\sigma^4} (W y^{2(\lambda)})' \epsilon \tag{28}$$

$$\frac{\partial^2 \log L}{\partial \lambda^2} = -\frac{1}{\sigma^2} \left[(I - \alpha_1 W) \frac{\partial y^{2(\lambda)}}{\partial \lambda} \right]' \left[(I - \alpha_1 W) \frac{\partial y^{2(\lambda)}}{\partial \lambda} \right] - \frac{1}{\sigma^2} \left[(I - \alpha_1 W) \frac{\partial^2 y^{2(\lambda)}}{\partial \lambda^2} \right]' \epsilon \tag{29}$$

$$\frac{\partial^2 \log L}{\partial \lambda \partial \sigma^2} = \frac{1}{\sigma^4} \left[(I - \alpha_1 W) \frac{\partial y^{2(\lambda)}}{\partial \lambda} \right]' \epsilon \tag{30}$$

$$\frac{\partial^2 \log L}{\partial (\sigma^2)^2} = \frac{n}{2\sigma^4} - \frac{1}{\sigma^6} \epsilon' \epsilon \stackrel{E}{=} -\frac{n}{2\sigma^4} \tag{31}$$

where $\frac{\partial^2 y^{2(\lambda)}}{\partial \lambda^2} = \frac{\lambda^2 y^{2\lambda} (\log y^2)^2 - 2\lambda y^{2\lambda} \log y^2 + 2y^{2\lambda} - 2}{\lambda^3}$

The terms of the outer product of the gradients are given by

$$\frac{\partial \log L}{\partial \alpha_0} \cdot \frac{\partial \log L}{\partial \alpha_0} = \left(\frac{1}{\sigma^2} \mathbf{1}' \epsilon \right)^2 \stackrel{E}{=} \frac{n}{\sigma^2} \tag{32}$$

$$\frac{\partial \log L}{\partial \alpha_0} \cdot \frac{\partial \log L}{\partial \alpha_1} = \frac{1}{\sigma^2} \mathbf{1}' \epsilon \left[\frac{1}{\sigma^2} (W y^{2(\lambda)})' \epsilon - \sum_{i=1}^{n} \frac{\omega_i}{1 - \alpha_1 \omega_i} \right] \tag{33}$$

$$\frac{\partial \log L}{\partial \alpha_0} \cdot \frac{\partial \log L}{\partial \lambda} = \frac{1}{\sigma^2}\mathbf{1}'\epsilon\Big[-\frac{1}{\sigma^2}\Big((I-\alpha_1 W)\frac{\partial y^{2(\lambda)}}{\partial \lambda}\Big)'\epsilon + \sum_{i=1}^{n}\log\left(y_i^2\right)\Big] \tag{34}$$

$$\frac{\partial \log L}{\partial \alpha_0} \cdot \frac{\partial \log L}{\partial \sigma^2} = \frac{1}{\sigma^2}\mathbf{1}'\epsilon\Big(-\frac{n}{2\sigma^2} + \frac{1}{2\sigma^4}\epsilon'\epsilon\Big) \stackrel{E}{=} \frac{nE(\epsilon_i^3)}{2\sigma^6} \tag{35}$$

$$\frac{\partial \log L}{\partial \alpha_1} \cdot \frac{\partial \log L}{\partial \alpha_1} = \Big[\frac{1}{\sigma^2}(Wy^{2(\lambda)})'\epsilon - \sum_{i=1}^{n}\frac{\omega_i}{1-\alpha_1\omega_i}\Big]^2 \tag{36}$$

$$\frac{\partial \log L}{\partial \alpha_1} \cdot \frac{\partial \log L}{\partial \lambda} = \Big[\frac{1}{\sigma^2}(Wy^{2(\lambda)})'\epsilon - \sum_{i=1}^{n}\frac{\omega_i}{1-\alpha_1\omega_i}\Big]\Big[-\frac{1}{\sigma^2}\Big((I-\alpha_1 W)\frac{\partial y^{2(\lambda)}}{\partial \lambda}\Big)'\epsilon + \sum_{i=1}^{n}\log\left(y_i^2\right)\Big] \tag{37}$$

$$\frac{\partial \log L}{\partial \alpha_1} \cdot \frac{\partial \log L}{\partial \sigma^2} = \Big[\frac{1}{\sigma^2}(Wy^{2(\lambda)})'\epsilon - \sum_{i=1}^{n}\frac{\omega_i}{1-\alpha_1\omega_i}\Big]\Big(-\frac{n}{2\sigma^2} + \frac{1}{2\sigma^4}\epsilon'\epsilon\Big) \tag{38}$$

$$\frac{\partial \log L}{\partial \lambda} \cdot \frac{\partial \log L}{\partial \lambda} = \Big[-\frac{1}{\sigma^2}\Big((I-\alpha_1 W)\frac{\partial y^{2(\lambda)}}{\partial \lambda}\Big)'\epsilon + \sum_{i=1}^{n}\log\left(y_i^2\right)\Big]^2 \tag{39}$$

$$\frac{\partial \log L}{\partial \lambda} \cdot \frac{\partial \log L}{\partial \sigma^2} = \Big[-\frac{1}{\sigma^2}\Big((I-\alpha_1 W)\frac{\partial y^{2(\lambda)}}{\partial \lambda}\Big)'\epsilon + \sum_{i=1}^{n}\log\left(y_i^2\right)\Big]\Big(-\frac{n}{2\sigma^2} + \frac{1}{2\sigma^4}\epsilon'\epsilon\Big) \tag{40}$$

$$\frac{\partial \log L}{\partial \sigma^2} \cdot \frac{\partial \log L}{\partial \sigma^2} = \Big(-\frac{n}{2\sigma^2} + \frac{1}{2\sigma^4}\epsilon'\epsilon\Big)^2 \stackrel{E}{=} \frac{n\big(E(\epsilon_i^4)-\sigma^4\big)}{4\sigma^8} \tag{41}$$

A.2 Chicago Community Areas

TABLE 13 Chicago community areas

#	Name	#	Name	#	Name	#	Name
1	Rogers Park	21	Avondale	41	Hyde Park	61	New City
2	West Ridge	22	Logan Square	42	Woodlawn	62	West Elsdon
3	Uptown	23	Humboldt park	43	South Shore	63	Gage Park
4	Lincoln Square	24	West Town	44	Chatham	64	Clearing
5	North Center	25	Austin	45	Avalon Park	65	West Lawn
6	Lake View	26	West Garfield Park	46	South Chicago	66	Chicago Lawn
7	Lincoln Park	27	East Garfield Park	47	Burnside	67	West Englewood
8	Near North Side	28	Near West Side	48	Calumet Heights	68	Englewood
9	Edison Park	29	North Lawndale	49	Roseland	69	Greater Grand Crossing
10	Norwood Park	30	South Lawndale	50	Pullman	70	Ashburn
11	Jefferson Park	31	Lower West Side	51	South Deering	71	Auburn Gresham
12	Forest Glen	32	Loop	52	East Side	72	Beverly
13	North Park	33	Near South Side	53	West Pullman	73	Washington Height
14	Albany Park	34	Armour Square	54	Riverdale	74	Mount Greenwood
15	Portage Park	35	Douglas	55	Hegewisch	75	Morgan Park
16	Irving Park	36	Oakland	56	Garfield Ridge	76	O'Hare
17	Dunning	37	Fuller Park	57	Archer Heights	77	Edgewater
18	Montclaire	38	Grand Boulevard	58	Brighton Park		
19	Belmont Cragin	39	Kenwood	59	McKinley Park		
20	Hermosa	40	Washington Park	60	Bridgeport		

A.3 Spatial Distribution of Returns and Squared Returns for Other Years

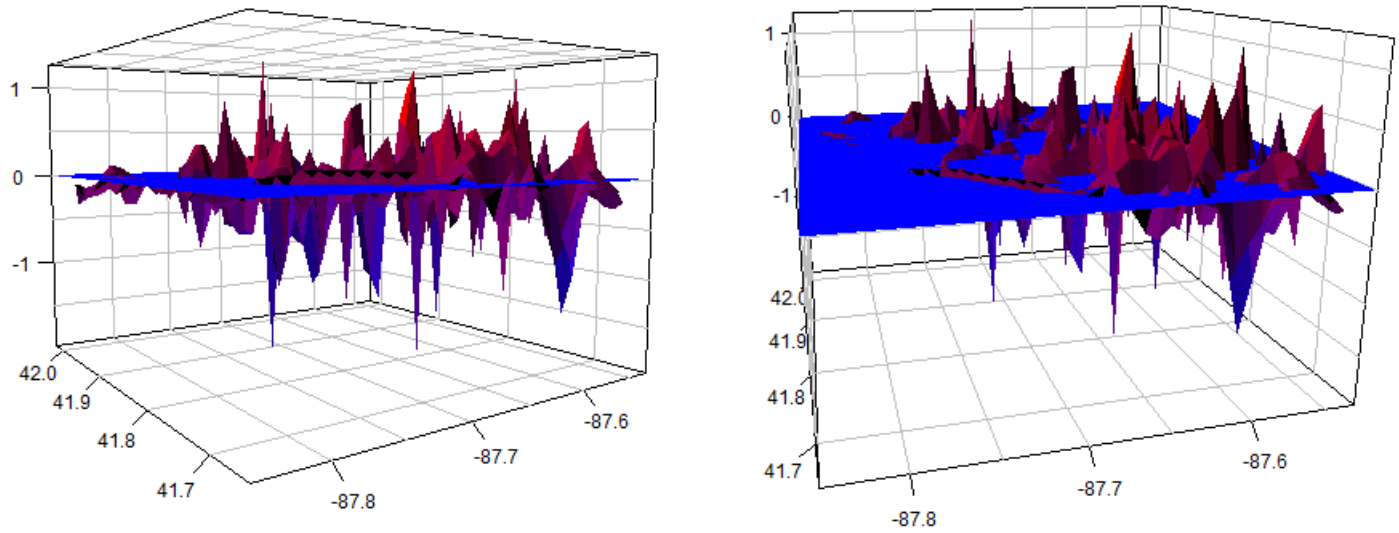

(a) Returns

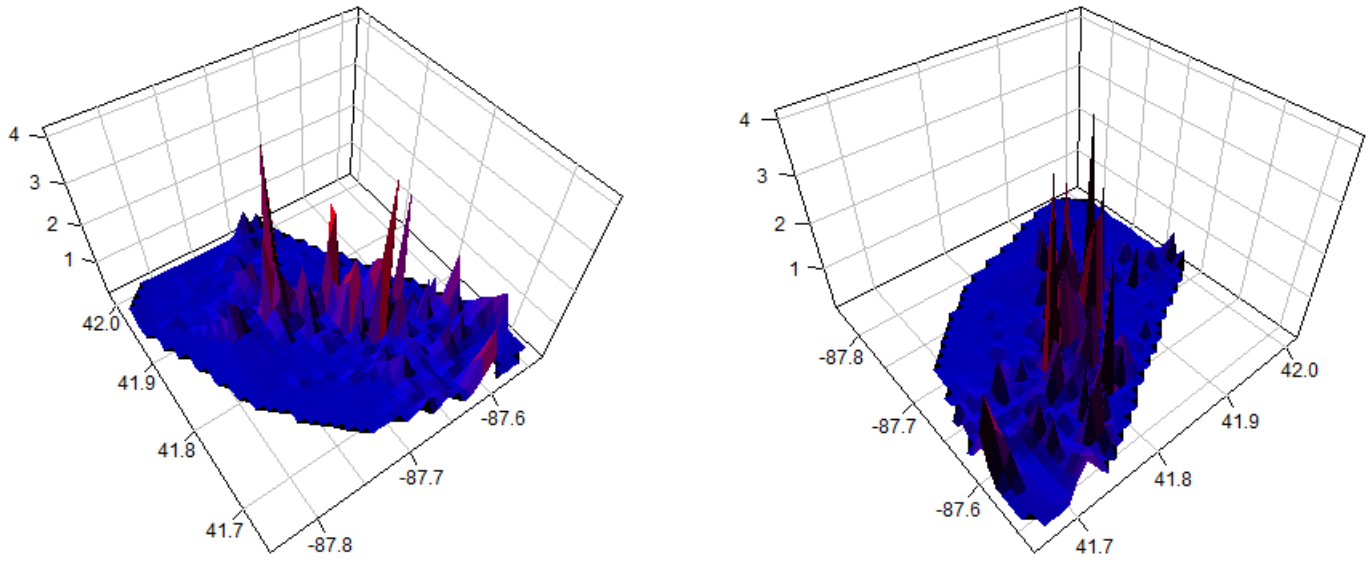

(b) Squared returns

FIGURE 9 Spatial distribution of returns and squared returns, 2010

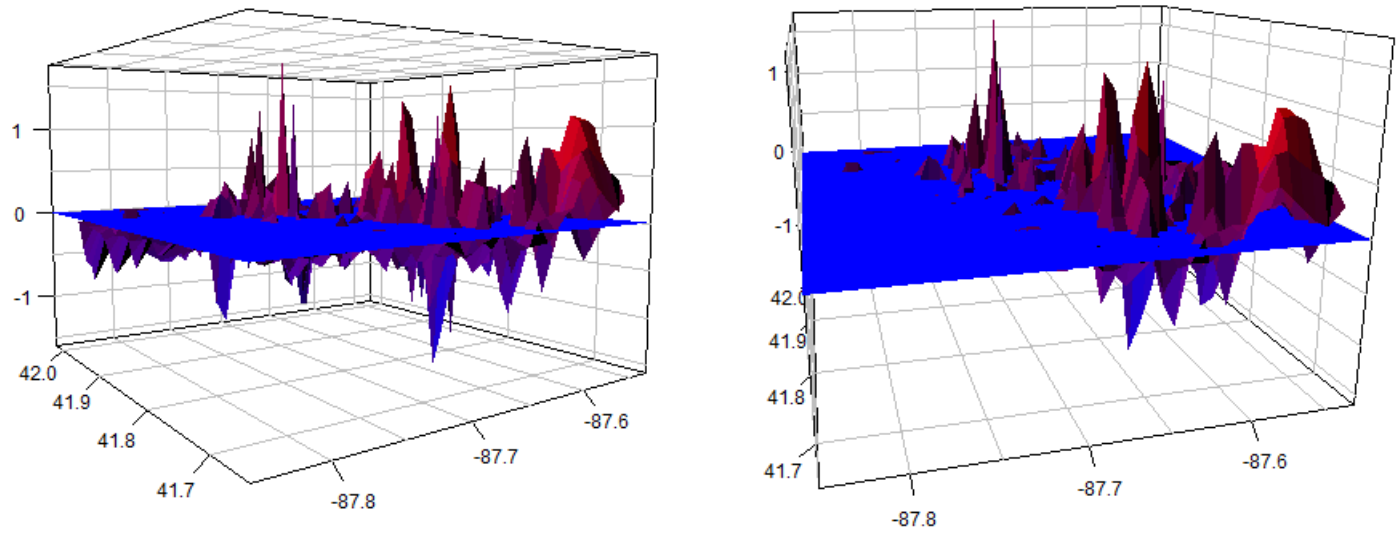

(a) Returns

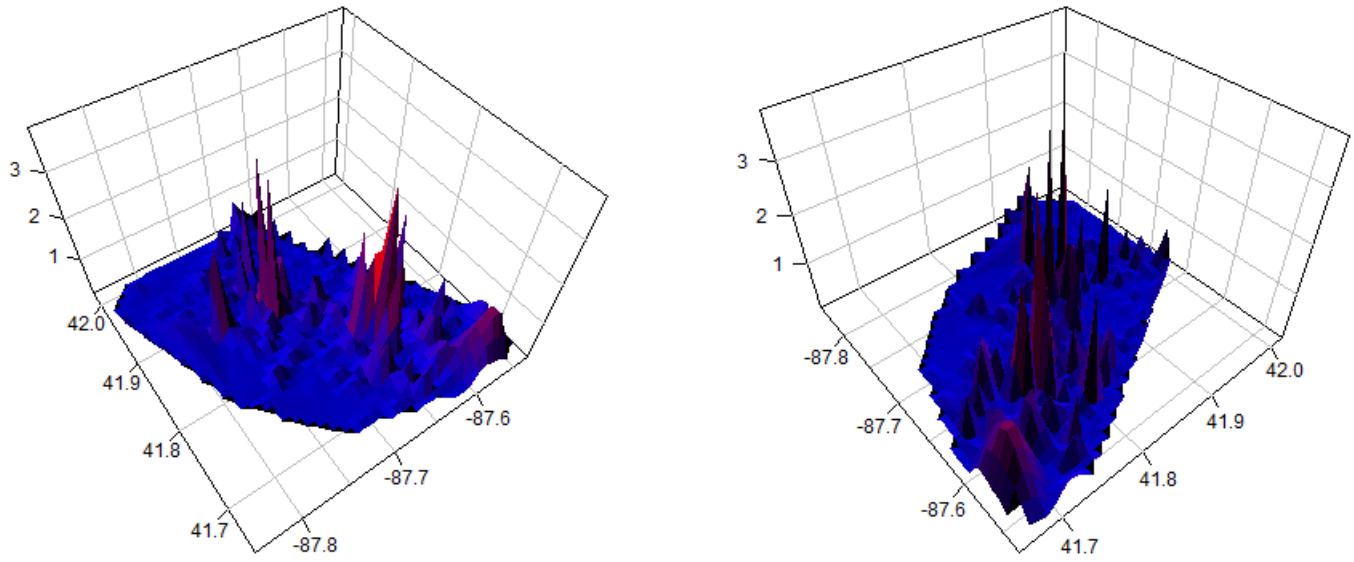

(b) Squared returns

FIGURE 10 Spatial distribution of returns and squared returns, 2011

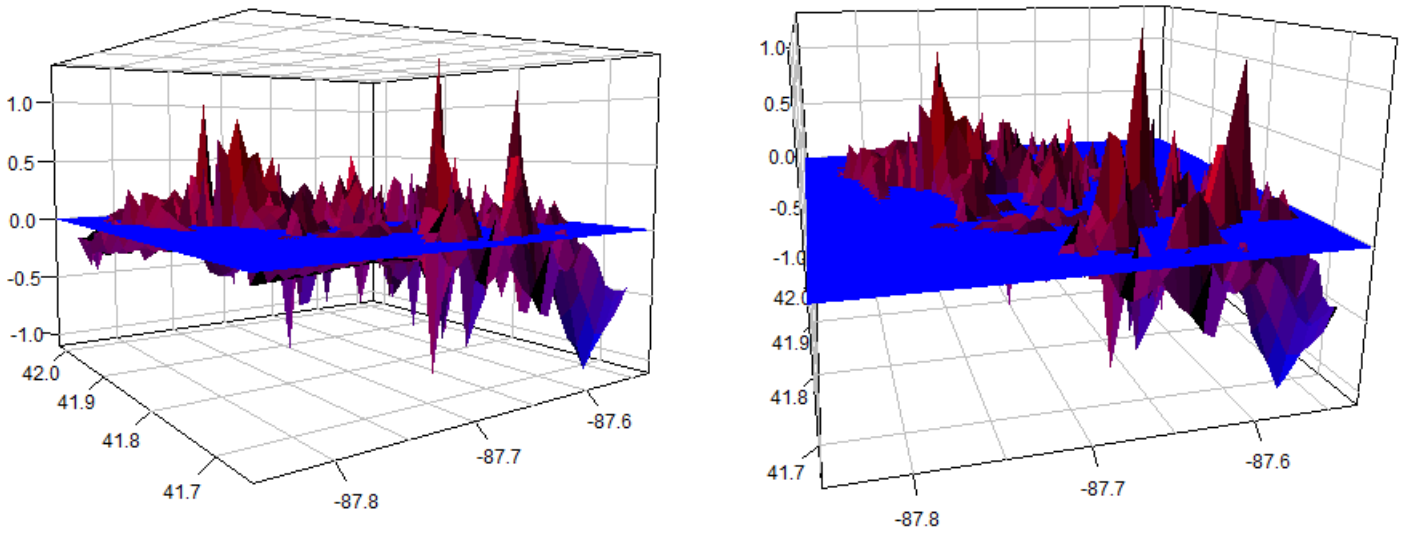

(a) Returns

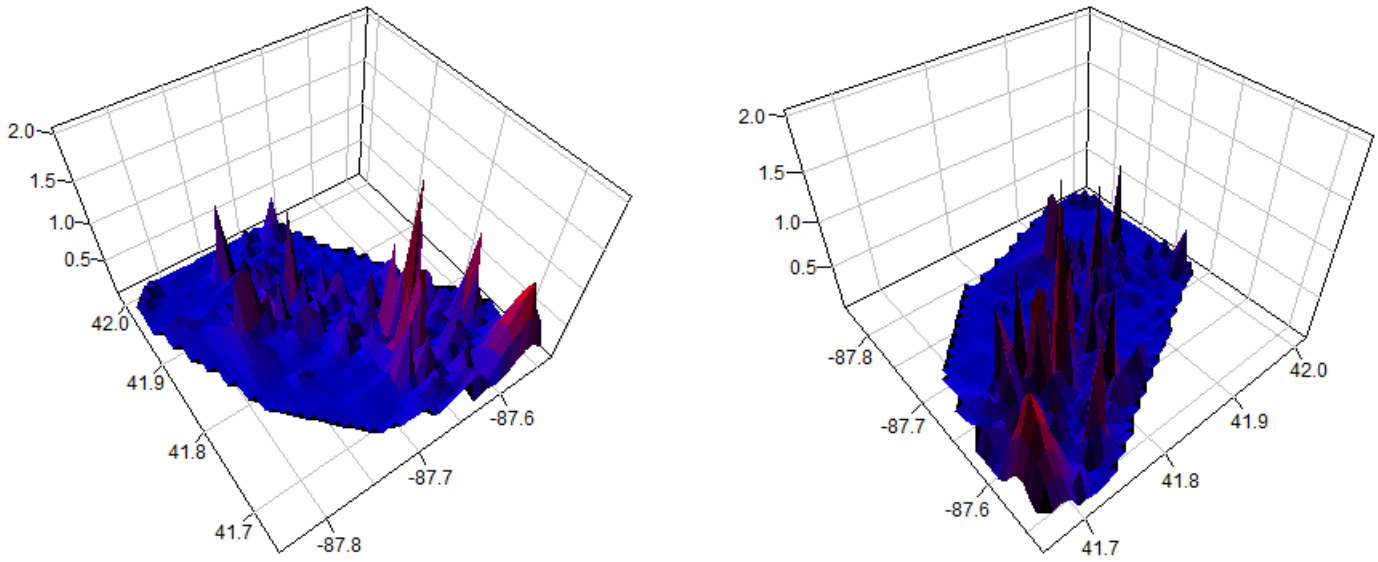

(b) Squared returns

FIGURE 11 Spatial distribution of returns and squared returns, 2012

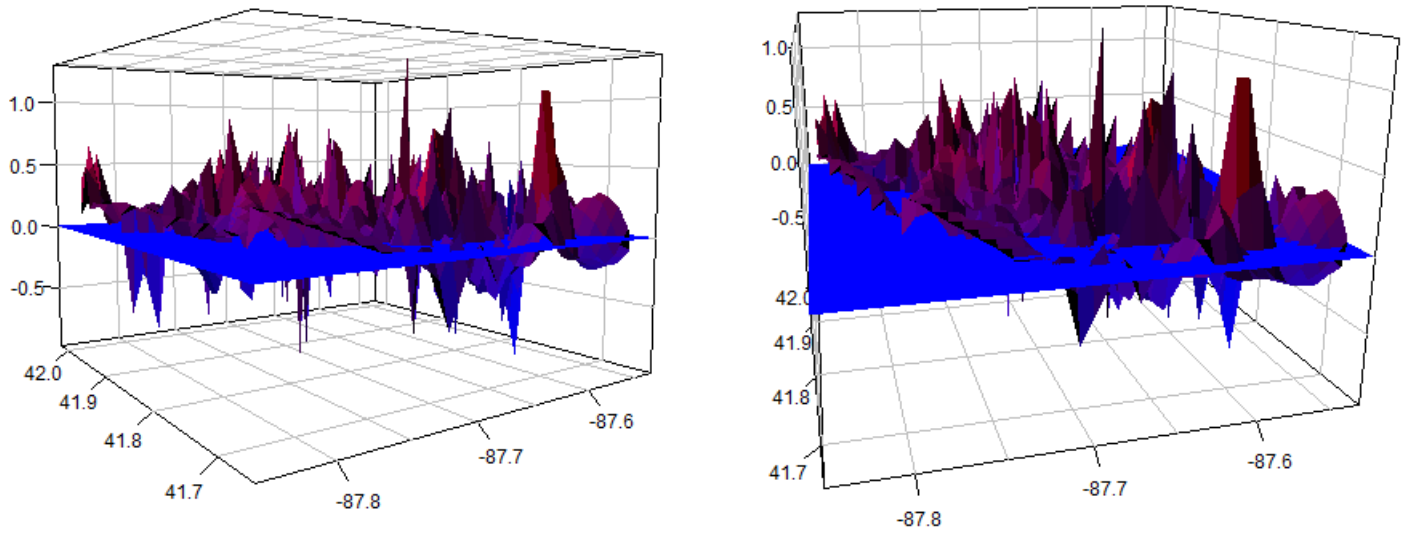

(a) Returns

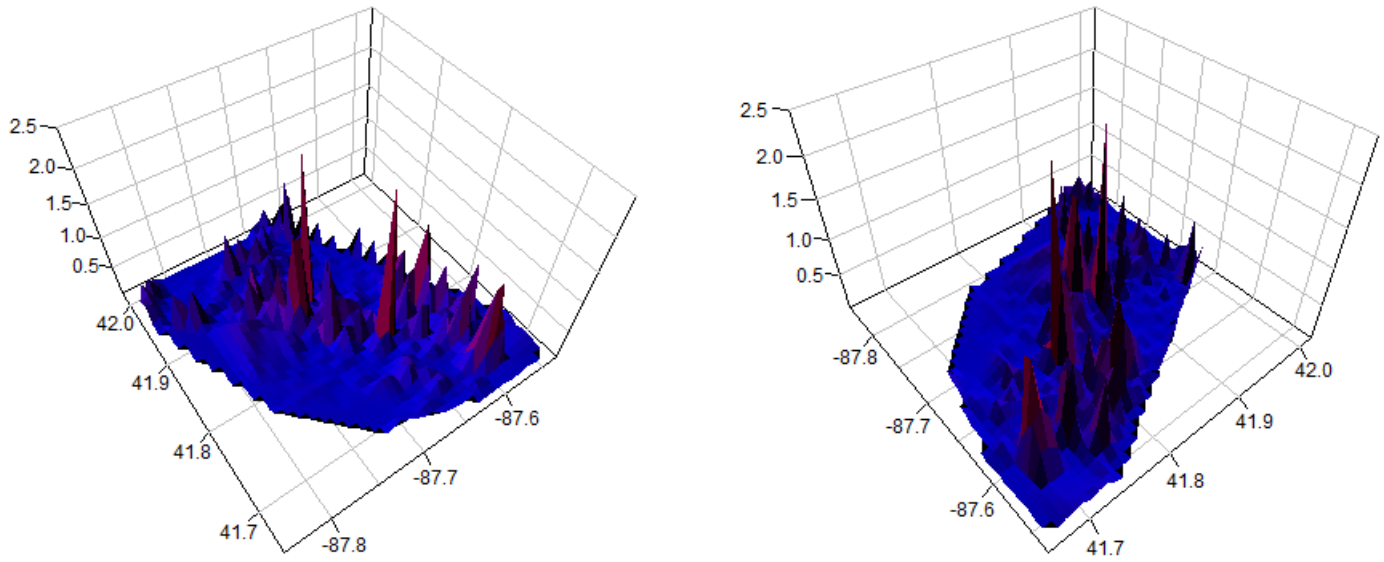

(b) Squared returns

FIGURE 12 Spatial distribution of returns and squared returns, 2013

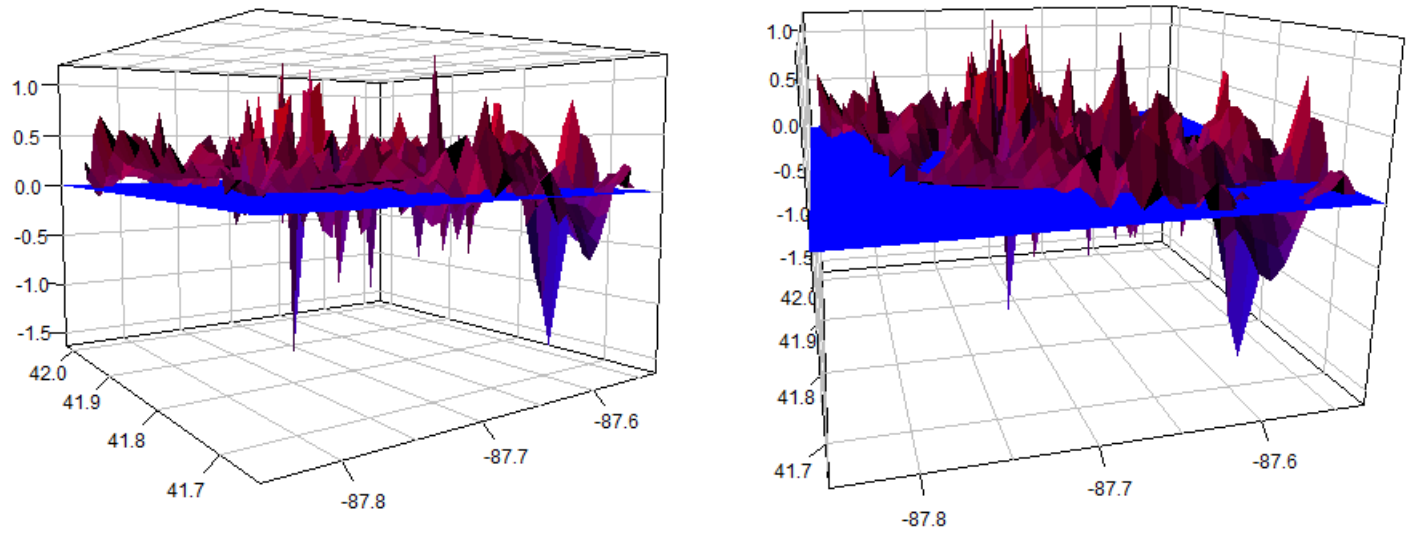

(a) Returns

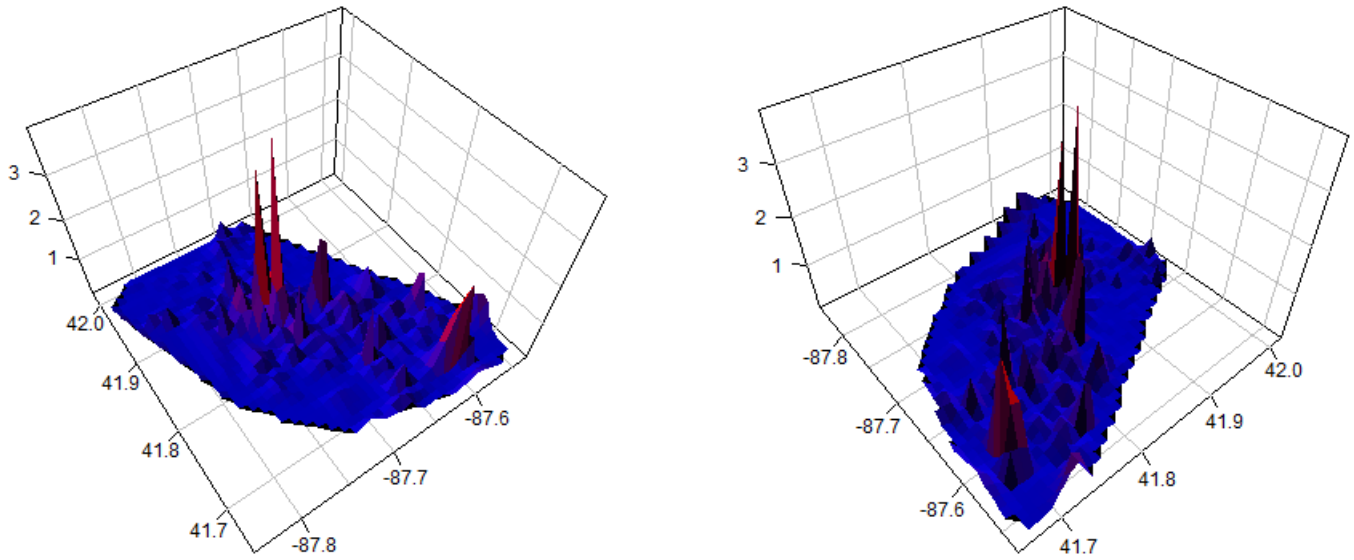

(b) Squared returns

FIGURE 13 Spatial distribution of returns and squared returns, 2014

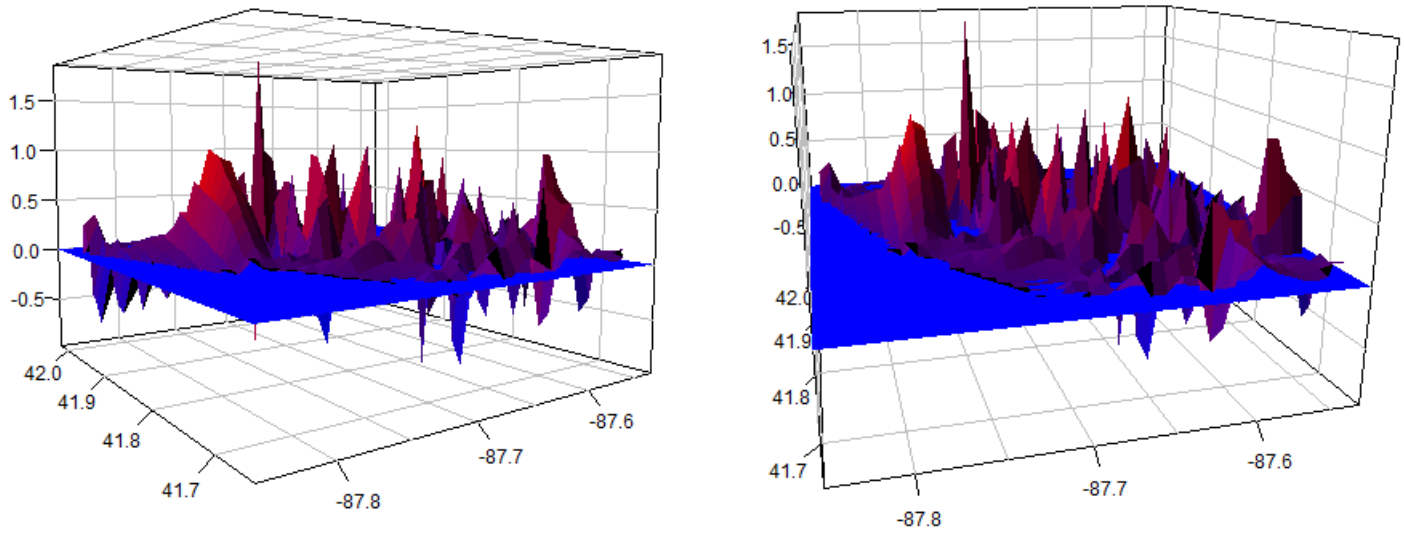

(a) Returns

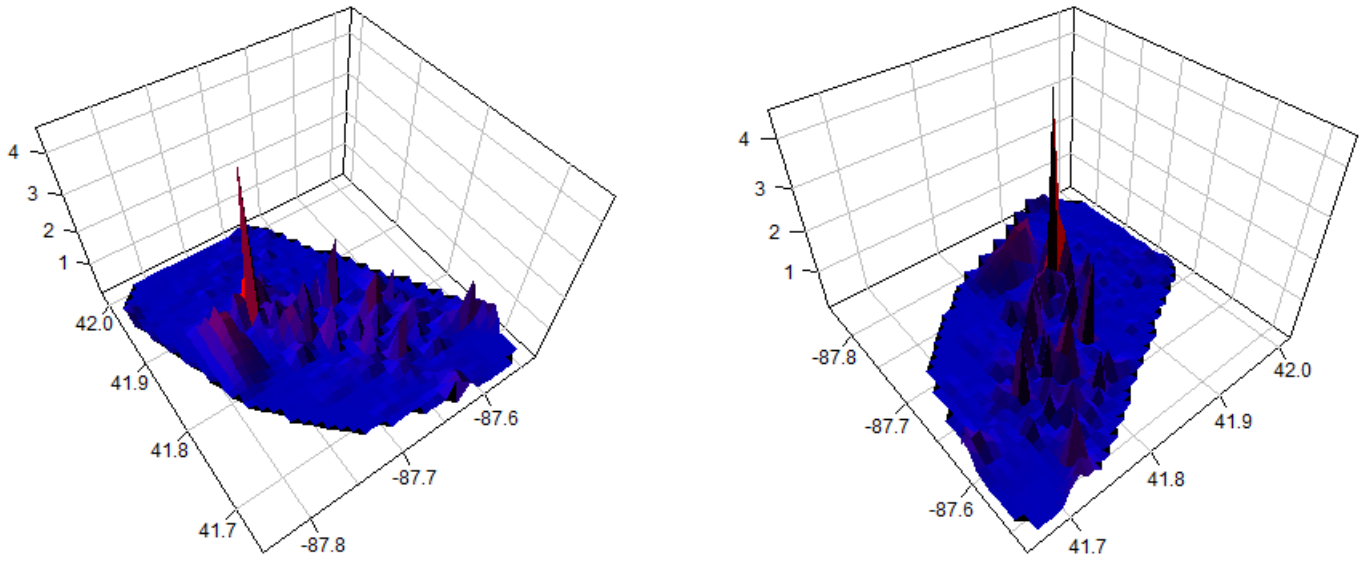

(b) Squared returns

FIGURE 14 Spatial distribution of returns and squared returns, 2015

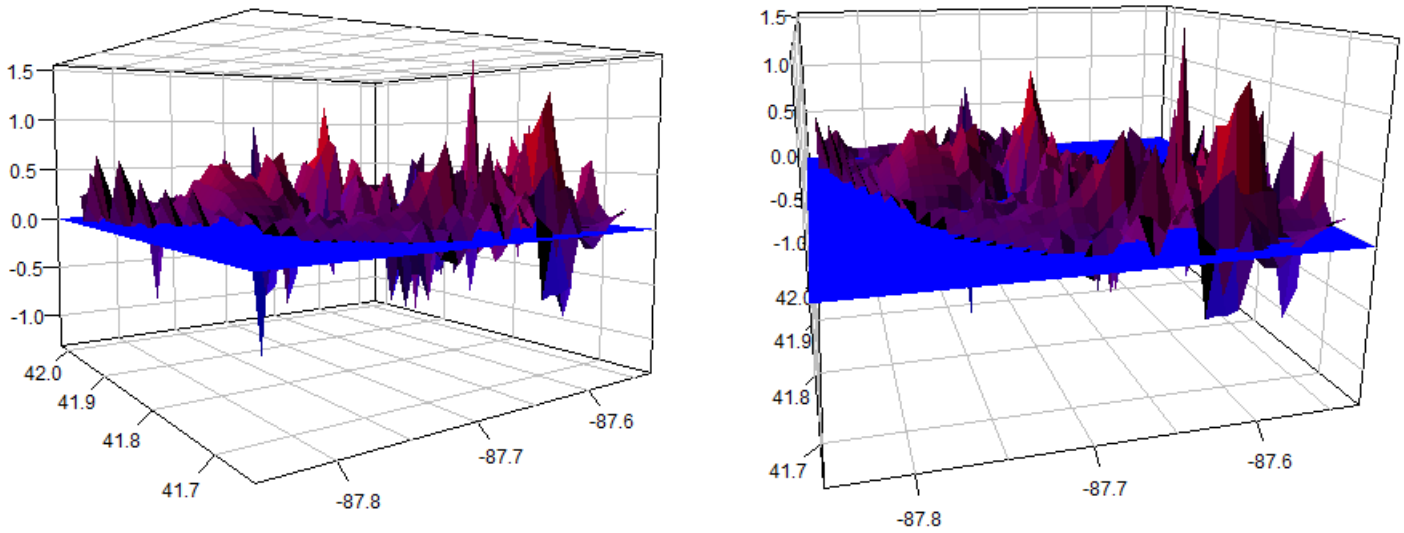

(a) Returns

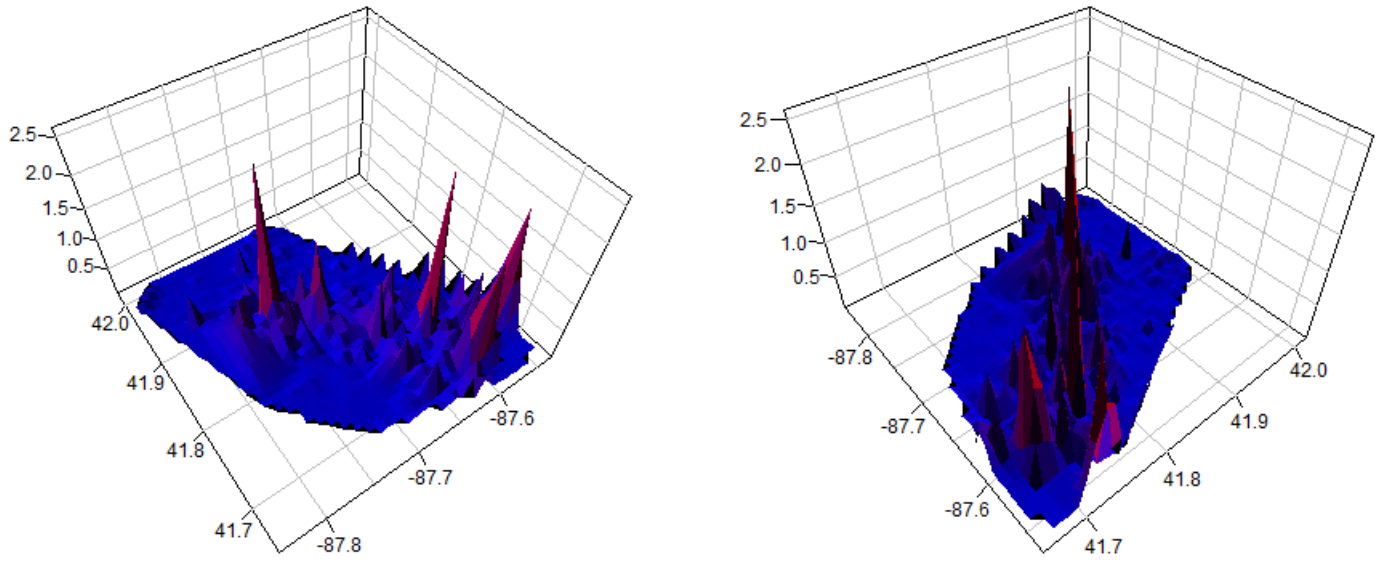

(b) Squared returns

FIGURE 15 Spatial distribution of returns and squared returns, 2016

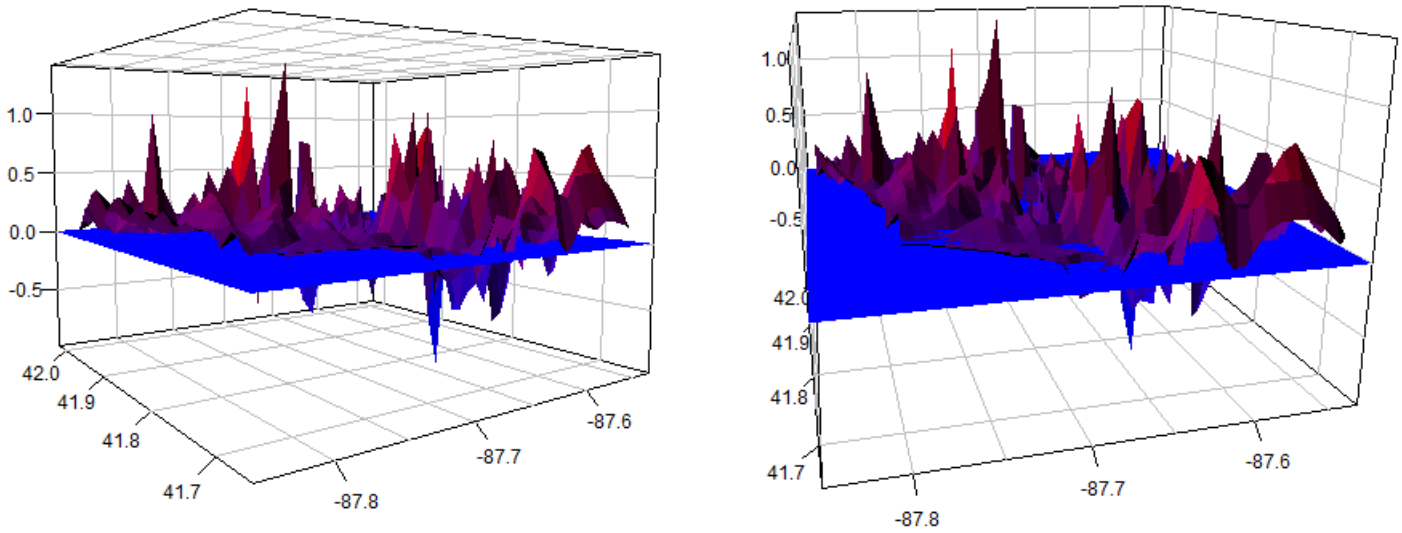

(a) Returns

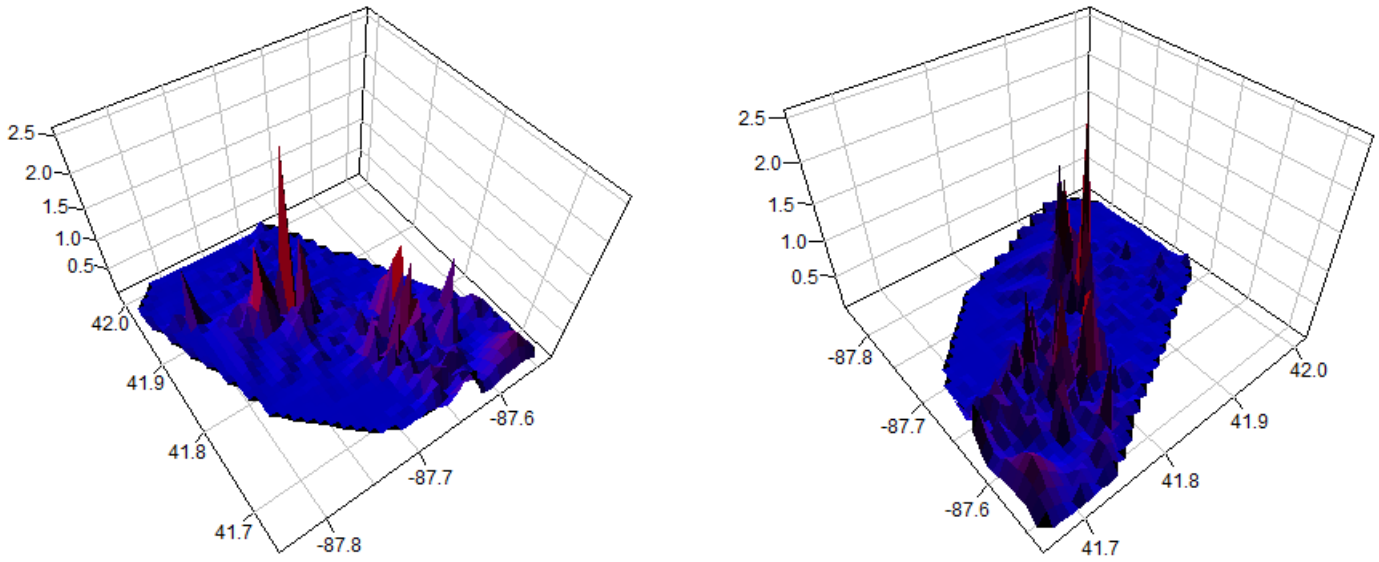

(b) Squared returns

FIGURE 16 Spatial distribution of returns and squared returns, 2018